J Math Imaging Vis
DOI 10.1007/s10851-016-0683-3

Nonlocal PDEs on Graphs: From Tug-of-War Games to Unified Interpolation on Images and Point Clouds

Abderrahim Elmoataz[1,2] · François Lozes[2] · Matthieu Toutain[3]

Received: 2 February 2016 / Accepted: 29 August 2016
© Springer Science+Business Media New York 2016

Abstract In this paper, we introduce a new general class of partial difference operators on graphs, which interpolate between the nonlocal ∞-Laplacian, the Laplacian, and a family of discrete gradient operators. In this context, we investigate an associated Dirichlet problem for this general class of operators and prove the existence and uniqueness of respective solutions. We show that a certain partial difference equation based on this class of operators recovers many variants of a stochastic game known as 'Tug-of-War' and extends them to a nonlocal setting. Furthermore, we discuss a connection with certain nonlocal partial differential equations. Finally, we propose to use this class of operators as general framework to solve many interpolation problems in a unified manner as arising, e.g., in image and point cloud processing.

Keywords PDEs on graph · Tug-of-War games · Nonlocal images and point clouds processing · Interpolation on point clouds · Colorization · Inpainting · Classification

✉ Abderrahim Elmoataz
abderrahim.elmoataz-billah@unicaen.fr

François Lozes
francois.lozes@unicaen.fr

Matthieu Toutain
matthieu.toutain@datexim.com

1 Laboratoire LIGIM, Université de Paris-Est Marne-La-Valée, Cité Descartes, Bâtiment Copernic - 5, bd Descartes, Champs sur Marne, 77454 Marne-la-Vallée Cedex 2, France

2 Université de Caen Normandie, GREYC Laboratory, 6 Boulevard Maréchal Juin, 14050 Caen Cedex, France

3 Datexim SAS, 51 Avenue de la Côte de Nacre, 14000 Caen Cedex, France

1 Introduction

Partial differential equations (PDEs) involving the p-Laplace and ∞-Laplace operators still generate a lot of interest both in the setting of Euclidean domains and on discrete graphs. These operators in their different forms, i.e., continuous, discrete, local, and nonlocal, are at the interface of many scientific fields as they are used to model many interesting phenomena, e.g., in mathematics, physics, engineering, biology, and economy. Some closely related applications can be found in image processing, computer vision, machine learning, and game theory, see, e.g., [3,9,15,26,28,38,51] and references therein.

The *continuous p-Laplacian* plays an important role in geometry and in the field of PDEs. For a comprehensive introduction and survey on these topics, we refer to [23,47] and references therein. Many inverse problems in image processing such as denoising, deconvolution, segmentation, inpainting are formulated as regularized minimization problems and are often solved based on PDEs and variational models which are related to the p-Laplacian. For $p = 2$, the well-known Tikhonov regularization is linked to Laplacian diffusion, while the case $p = 1$ corresponds to the total variation regularization.

The *game p-Laplacian* is a variant of the p-Laplacian which was recently introduced in connection with a stochastic game called Tug-of-War with noise [60]. For $p = 1$, this operator is related to the mean curvature flow, which has numerous applications ranging from free boundary problems in material sciences and computational fluid dynamics to filtering, inpainting, and segmentation in image processing and computer vision [56,64]. For $1 < p < \infty$, the game p-Laplacian can be expressed as a convex combination of the 1-Laplacian and the ∞-Laplacian [38]. For the special case of $p = \infty$, this operator has also been used in

Published online: 10 September 2016

several applications in image processing, computer vision, surface reconstruction, and image inpainting [25,32]. Indeed, game theoretic methods have recently emerged as a novel approach to study nonlinear elliptic PDEs. In particular, Tug-of-War games related to PDEs based on the p-Laplace and the ∞-Laplace equation have emerged, e.g., see [50,59] and references therein. One way to establish the link between these PDEs and the Tug-of-War game is to show that there exists a value function of the respective game which satisfies a dynamic programming principle (DPP). This DPP is generally a statistical functional involving the min, max, and mean operators. It can be interpreted as a local approximation of the PDE in question.

Finally, we would also like to mention the *nonlocal p-Laplacian* and the *fractional Laplacian*. The interest for these operators has constantly increased over the last few years. They arise in a number of applications such as continuum mechanics, phase transition phenomena, population dynamics, image processing, and game theory (see [3,4,34] and references therein). In image processing, regularization based on the nonlocal p-Laplacian [33] is related to nonlocal total variation or the nonlocal mean proposed by Buades et al. [14]. In general, nonlocal regularization methods have shown their superiority over classical models since local smoothness is not mandatory. In particular, they are well known for their ability to preserve both geometric and repetitive structures in images [5,31].

On the other hand, discrete Laplacian operators have been extensively used in image processing and in machine learning for clustering or dimension reduction [18,71]. The *graph p-Laplacian*, which is a generalization of the conventional discrete Laplacian, has started to attract attention in mathematics, machine learning, image and manifold processing community. For $p \neq 2$, the graph p-Laplacian has been studied in relation to the p-cheeger cut [36] and data clustering and for semi-supervised classification [74]. Meanwhile, partial difference equations (PdEs) on graphs involving the p-Laplacian have been investigated as a subject of its own interest, dealing with existence and qualitative behavior of respective solutions, see, e.g., [43,55,57].

1.1 Our Previous Works

In previous works, we have introduced a framework for partial difference equations which enables us to translate and adapt continuous PDEs and variational methods to the setting of graphs [11,27,68]. Conceptually, the idea of introducing PdEs is to mimic continuous PDEs on graph structures by consistently adapting important mathematical concepts, e.g., integration and differentiation. By doing so, one is able to directly translate most of the established techniques for PDEs and in particular for the p-Laplace operator to graphs. Moreover, in case of evolution PdEs this framework provides models in which spatial integration and temporal evolution can be handled separately. Indeed, in this case there is no need for a spatial discretization and one gains a unification of local and nonlocal models [28]. In our previous works, we have also introduced a family of p-Laplacian operators (isotropic and anisotropic) on graphs in divergence form [11] within this framework.

In [11,27], we have introduced nonlocal regularization on weighted graphs of arbitrary topology. In particular, it was shown that these regularization methods lead to a family of discrete and semi-discrete diffusion processes based on discrete p-Laplacian operators. These processes, parametrized both by the graph structure (topology and geometry) and by the degree of smoothness p, allow to perform several filtering tasks such as denoising, simplification, or clustering. Moreover, local and nonlocal image regularizations are formalized within the same framework, which corresponds to the transcription of local or nonlocal regularization proposed in [34]. Based on the same ideas, we have proposed PdEs for morphological processes on graphs to transcribe continuous morphological PDEs such as dilation and erosion [68]. The study of well-posedness of the Eikonal equation on graphs has recently been reported in [22]. Furthermore, we have proposed the adaptation of both nonlocal ∞-Laplacian [25] and game p-Laplacian for $2 \leq p \leq \infty$ on graphs [26].

In [69], we proposed to adapt and solve a general equation, of type ∞-Poisson and Hamilton–Jacobi, on weighted graphs. This equation was used to approximate generalized distance on weighted graphs, but also to perform image segmentation and data classification. We showed the connections between this particular equation and Tug-of-War games, related to ∞-Laplacian with gradient terms.

The operator we proposed in this last article corresponds to a particular case of the one we proposed later in [29], which we present in the next section. In this article, we have proposed a family of p-Laplacian and ∞-Laplacian type operator, and we studied both the parabolic and elliptic equations, proving existence and uniqueness of the solution to the associated Dirichlet problem. The case $p = \infty$ corresponds to the operator in [69]. We also showed the connections with Tug-of-War games and the elliptic equation, related to the ∞-Laplacian.

1.2 Main Contributions

This paper follows our previous work.

Let G be a weighted graph, V the set of vertices of G, and $f : V \to \mathbb{R}$ a function of the Hilbert space $\mathcal{H}(V)$ of real-valued functions defined on the graph vertices. In [29], we proposed a general p-Laplacian with gradient terms on weighted graphs $\mathcal{L}_{w,p} : \mathcal{H}(V) \to \mathbb{R}$, defined as:

$$\begin{cases} \alpha(u)\|\nabla_w^+(f)(u)\|_{p-1}^{p-1} - \beta(u)\|\nabla_w^-(f)(u)\|_{p-1}^{p-1}, & 2 \le p < \infty, \\ \alpha(u)\|\nabla_w^+(f)(u)\|_\infty - \beta(u)\|\nabla_w^-(f)(u)\|_\infty, & p = \infty, \end{cases} \tag{1}$$

where $\alpha, \beta : V \to [0, 1]$, $\alpha(u) + \beta(u) = 1$, and ∇_w^+ and ∇_w^- are the weighted upwind gradients, defined later in this paper. We showed in [29] that this operator enables the recovery of the p-Laplacian, the ∞-Laplacian (for $p = \infty$), and morphological operators on graphs. We also showed that this operator corresponds to the value functions of Tug-of-War games in the discrete setting of weighted graphs. In [69], we used a particular case of (1) with $p = \infty$ to propose a hybrid ∞-Poisson and Hamilton–Jacobi equation in the setting of graphs:

$$\begin{cases} \mathcal{L}_{w,\infty}(f)(u) = h(u), & u \in \mathcal{A}, \\ f(u) = g(u), & u \in \partial\mathcal{A}, \end{cases} \tag{2}$$

with $\mathcal{A}$ a subset of V and $\partial\mathcal{A}$ its boundaries (defined later in the article).

We also showed in [69] the relation between this equation and Tug-of-War games.

In this paper, we propose a new formulation of operator of p-Laplacian type, and we study a novel general class of PdEs, using the proposed operator on weighted graphs. These equations are based on finite difference operators which interpolate between two discrete upwind gradients and the p-Laplacian operator on graphs. This operator is defined as follows:

$$\Delta_{\alpha,\beta,\gamma} f \;=\; \alpha||\nabla_w^+ f||_\infty - \beta||\nabla_w^- f||_\infty + \gamma\Delta_{w,2} f, \tag{3}$$

where $\alpha, \beta, \gamma \in \mathbb{R}^+$ and $\alpha + \beta + \gamma = 1$. Depending on the values of α, β, and γ, we show that we are able to recover the discrete analogues of many local and nonlocal PDEs involving the conventional Laplacian, the ∞-Laplacian, and the p-Laplacian with and without additional gradient terms. The advantage of the involved family of operators is its adaptivity with respect to potential applications, i.e., to handle many local and nonlocal interpolation problems in image and data processing within the same unified framework, e.g., inpainting, colorization, and semi-supervised clustering.

The main contributions in this paper are the following:

- We propose a novel family of operators on graphs, which unifies our previous works and allows to translate many interesting models continuous local as well as nonlocal PDEs to the graph framework.
- We investigate an associated Dirichlet problem on graphs and prove the existence and uniqueness of respective solutions.
- We establish a connection to many local Tug-of-War games:
  - Tug-of-War related to ∞-Laplacian equation,
  - Tug-of-War related to ∞-Laplacian equation with gradient terms,
  - Tug-of-War with noise related to game p-Laplacian equation,
  - Tug-of-War with noise related to game p-Laplacian equation with gradient terms.
- Then we show that the elliptic equation involving our class of operator can be interpreted as a new nonlocal formulation of these games.

Furthermore, in order to solve the associated Dirichlet problem in the setting of discrete graphs we propose an algorithm which can be used to unify interpolation tasks on both conventional images and point cloud data. As we will show on real-world data, this algorithm might be useful in particular for:

- inpainting of images and 3D point clouds.
- colorization of 3D point clouds.
- semi-supervised classification of databases (represented as high-dimensional point clouds).

1.3 Paper Organization

The rest of this work is organized as follows: In Sect. 2, we provide basic definitions and notations, which are used throughout this work. Furthermore, we recall our previous works on PdEs on graphs and the p-Laplacian on graphs. In Sect. 3, we derive a novel partial difference operator which interpolates between the graph p-Laplacian, the graph ∞-Laplacian, and discrete gradient operators. Then, we study an associated Dirichlet problem and prove the existence and uniqueness of respective solutions. Furthermore, we present and discuss the connections between nonlocal continuous PDEs and Tug-of-War games. Section 4 presents several applications and interpolation problems on real-world images and point clouds. Finally, a short discussion in Sect. 5 concludes this paper.

2 Partial Difference Operators on Graphs

In this section, we introduce the basic notations used throughout this paper. Additionally, we recall various definitions of difference operators on weighted graphs from previous works in order to define in this context derivatives, the p-Laplace operator, and some morphological operators on graphs. More details on these operators can be found in [11,27,68].

2.1 Notations

Let us consider the general situation in which any discrete domain can be viewed as a weighted graph. A weighted graph $G = (V, E, w)$ consists of a finite set V of $m \in \mathbb{N}$ vertices and of a finite set $E \subseteq V \times V$ of edges. Let $(u, v) \in E$ be an edge that connects two vertices $u \in V$ and $v \in V$. An graph is weighted if it is associated with a weight function $w : V \times V \to [0, 1]$. A weighted graph is denoted as undirected if this weight function satisfies $w(u, v) = w(v, u)$ for all $(u, v) \in V \times V$. Note that the weight function often represents a similarity measure between two vertices of the graph based on an appropriate feature. If we use the notation $u \sim v$ to denote two adjacent vertices, we can give an alternative characterization of the edge set with respect to the weight function w by $E = \{(u, v) \mid w(u, v) > 0\}$. The degree of a vertex u is defined as $\delta_w(u) = \sum_{v\sim u} w(u, v)$, while the neighborhood of a vertex u (i.e., the set of vertices adjacent to u) is denoted as $N(u)$. In this paper, we consider only weighted graphs which are connected, undirected, and without self-loops or multiple edges.

Let $\mathcal{H}(V)$ be the Hilbert space of real-valued functions defined on the graph vertices. Each function $f : V \to \mathbb{R}$ of $\mathcal{H}(V)$ assigns a real value $f(u)$ to each vertex $u \in V$. Similarly, let $\mathcal{H}(E)$ be the Hilbert space of real-valued functions defined on the edges of the graph. It gets clear that the two spaces can be endowed with the following inner products: $\langle f, g\rangle_{\mathcal{H}(V)} = \sum_{u\in V} f(u)g(u)$ for $f, g \in \mathcal{H}(V)$, and $\langle F, G\rangle_{\mathcal{H}(E)} = \sum_{(u,v)\in E} F(u, v)G(u, v)$ for $F, G \in \mathcal{H}(E)$.

For a given function $f : V \to \mathbb{R}$, the l^p norm is given by

$$\|f\|_p = \Big(\sum_{u\in V} |f(u)|^p\Big)^{1/p}, \quad 1 \leqslant p < \infty$$
$$\|f\|_\infty = \max_{u\in V}\big(|f(u)|\big), \qquad p = \infty.$$

Let $\mathcal{A}$ be a set of connected vertices with $\mathcal{A} \subset V$. We denote by $\partial\mathcal{A}$ the boundary set of $\mathcal{A}$:

$$\partial\mathcal{A} = \{u \in \mathcal{A}^c : \exists v \in \mathcal{A} \text{ with } (u, v) \in E\}, \tag{4}$$

for which $\mathcal{A}^c = V \setminus \mathcal{A}$ is the complement of $\mathcal{A}$.

2.2 Weighted Finite Difference Operators

The (possibly nonlocal) *weighted finite difference operator* of a function $f \in \mathcal{H}(V)$, denoted by $\mathcal{G}_w : \mathcal{H}(V) \to \mathcal{H}(E)$, is defined on a pair of vertices $(u, v) \in E$ as :

$$(\mathcal{G}_w f)(u, v) = \sqrt{w(u, v)}\,(f(v) - f(u))\,. \tag{5}$$

Note that this difference operator is linear and antisymmetric.

The *adjoint* of the difference operator in (5), denoted by $\mathcal{G}_w^* : \mathcal{H}(E) \to \mathcal{H}(V)$, is a linear operator which can be characterized by $\langle \mathcal{G}_w f, H\rangle_{\mathcal{H}(E)} = \langle f, \mathcal{G}_w^* H\rangle_{\mathcal{H}(V)}$ for all $f \in \mathcal{H}(V)$ and all $H \in \mathcal{H}(E)$. Using the definitions of the finite weighted difference operator and the inner products of $\mathcal{H}(V)$ and $\mathcal{H}(E)$, the adjoint operator $\mathcal{G}_w^*$ of a function $H \in \mathcal{H}(E)$ can be expressed at a vertex $u \in V$ by the following expression:

$$(\mathcal{G}_w^* H)(u) = \sum_{v\sim u} \sqrt{w(u, v)}(H(v, u) - H(u, v)). \tag{6}$$

Based on this adjoint, the *divergence operator* $\operatorname{div}_w = -\mathcal{G}_w^*$ measures the net outflow of a function of $\mathcal{H}(E)$ at each vertex of the graph. Note that for every function $H \in \mathcal{H}(E)$, the total divergence over the entire set of vertices is zero. Based on the previous definitions, it can be easily shown that $\sum\limits_{(u,v)\in E} \mathcal{G}_w f(u, v) = 0$ for $f \in \mathcal{H}(v)$, and $\sum\limits_{u\in V} \operatorname{div}_w F(u) = 0$ for $F \in H(E)$.

The *weighted directional derivative* of f at a vertex u along the edge (u, v) is defined as:

$$\partial_v f(u) = \sqrt{w(u, v)}\big(f(v) - f(u)\big). \tag{7}$$

Furthermore, we can introduce two *discrete upwind derivatives* $\partial_v^\pm : \mathcal{H}(V) \to \mathcal{H}(E)$ by the following expressions:

$$\partial_v^\pm f(u) = \sqrt{w(u, v)}\big(f(v) - f(u)\big)^\pm, \tag{8}$$

with $(x)^+ = \max(0, x)$, $(x)^- = -\min(0, x) = \max(0, -x)$.

The (possibly nonlocal) *weighted gradient* of a given function $f \in \mathcal{H}(V)$, denoted as $\nabla_w : \mathcal{H}(V) \to \mathcal{H}(V)^m$, is defined on a vertex $u \in V$ as the vector of all weighted directional derivatives in (7) with respect to the set of vertices V:

$$(\nabla_w f)(u) = (\partial_v f(u))_{v\in V}\,. \tag{9}$$

Analogously, using the notation in (8) we can introduce two *weighted upwind gradients* by:

$$(\nabla_w^\pm f)(u) = \big(\partial_v^\pm f(u)\big)_{v\in V}\,. \tag{10}$$

A family of *gradient norm operators* $||\big(\nabla_w f\big)||_p : \mathcal{H}(V) \to \mathcal{H}(V)$ with $1 \leqslant p < \infty$ is given for a function $f \in \mathcal{H}(V)$ as:

$$||\big(\nabla_w f\big)(u)||_p = \left[\sum_{v\sim u} \sqrt{w(u, v)}^p |f(v) - f(u)|^p\right]^{\frac{1}{p}}. \tag{11}$$

Analogously, a family of *upwind gradient norm operators* $||\big(\nabla_w^\pm f\big)||_p : \mathcal{H}(V) \to \mathcal{H}(V)$ with $1 \leqslant p < \infty$ for a function $f \in \mathcal{H}(V)$ is defined as:

$$||\big(\nabla_w^{\pm} f\big)(u)||_p = \left[\sum_{v\sim u} \sqrt{w(u,v)}^{\,p} |(f(v)-f(u))^{\pm}|^p\right]^{\frac{1}{p}}. \tag{12}$$

In the case $p = \infty$, the *gradient norm operator* $||\nabla_w f||_\infty : \mathcal{H}(V) \to \mathcal{H}(V)$ for a function $f \in \mathcal{H}(V)$ is defined as:

$$||\big(\nabla_w f\big)(u)||_\infty = \max_{v\sim u}\Big(\sqrt{w(u,v)}\big(f(v)-f(u)\big)\Big). \tag{13}$$

Similarly, two *upwind gradient norm operators* $||\nabla_w^{\pm} f||_\infty : \mathcal{H}(V) \to \mathcal{H}(V)$ for a function $f \in \mathcal{H}(V)$ can be defined as:

$$||\big(\nabla_w^{\pm} f\big)(u)||_\infty = \max_{v\sim u}\Big(\sqrt{w(u,v)}\big(f(v)-f(u)\big)^{\pm}\Big). \tag{14}$$

Note that the previously introduced operators allow to measure the regularity of a function f around a vertex u.

An interesting relation between the weighted gradient norm operator and its upwind variants is given for a function $f \in \mathcal{H}(V)$ by:

$$||\big(\nabla_w f\big)(u)||_p^p = ||\big(\nabla_w^{+} f\big)(u)||_p^p + ||\big(\nabla_w^{-} f\big)(u)||_p^p, \tag{15}$$

and one can directly deduce that

$$||\big(\nabla_w^{\pm} f\big)(u)||_p^p \leqslant ||\big(\nabla_w f\big)(u)||_p^p. \tag{16}$$

Thus, the latter operators provide a slightly finer characterization of the gradient. For instance, one can remark that $||\big(\nabla_w^{-} f\big)(u)||_p$ is always zero if f has a local minimum at u.

The upwind discrete gradient ∇_w^- has been used in [22,67] to adapt the Eikonal equation on weighted graphs and to study its well-posedness (existence and uniqueness of respective solutions) with applications in image processing and machine learning. Moreover, this family of gradients can be used to construct several nonlocal regularization functionals on graphs, which can be interpreted as extensions of the total variation regularization on graphs. For instance:

$$\begin{aligned}
J_{p,w}(f) &= \sum_{u\in V} ||(\nabla_w f)(u)||_p^p, \quad 1 \leqslant p < \infty,\\
J_{\infty,w}(f) &= \sum_{u\in V} ||(\nabla_w f)(u)||_\infty,\\
J_{p,w}^{\pm}(f) &= \sum_{u\in V} ||(\nabla_w^{\pm} f)(u)||_p^p, \quad 1 \leqslant p < \infty,\\
J_{\infty,w}^{\pm}(f) &= \sum_{u\in V} ||(\nabla_w^{\pm} f)(u)||_\infty.
\end{aligned} \tag{17}$$

These gradients were also used to approximate certain continuous Hamilton–Jacobi equations on a discrete domain [22,68]. For example, given two functions $f, \mu : \Omega \subset \mathbb{R}^n \to \mathbb{R}$, then any continuous equation of the form:

$$\frac{\partial f(x,t)}{\partial t} = \mu(x)||\nabla f(x,t)||_p, \tag{18}$$

can be numerically approximated in a discrete setting as:

$$\frac{\partial f(u,t)}{\partial t} = \mu^+(u)||\big(\nabla_w^+ f\big)(u,t)||_p - \mu^-(u)||\big(\nabla_w^- f\big)(u,t)||_p. \tag{19}$$

In particular, if $\mu \equiv 1$, $p = \infty$, and if we employ a forward Euler time discretization (with a time step size of $\Delta t = 1$) this equation can be rewritten as:

$$f^{k+1}(u) = f^k(u) + ||\big(\nabla_w^+ f^k\big)(u)||_\infty, \tag{20}$$

with $f^k(u) = f(u, k\Delta t)$. This can be interpreted as a single iteration of the following *nonlocal dilation*-type operator:

$$f^{k+1}(u) = \mathrm{NLD}\big(f^k\big)(u), \tag{21}$$

where $\mathrm{NLD} : \mathcal{H}(V) \to \mathcal{H}(V)$ is defined as:

$$\mathrm{NLD}\big(f\big)(u) = f(u) + \max_{u\sim v}\Big(\sqrt{w(u,v)}\big(f(v)-f(u)\big)^+\Big). \tag{22}$$

Similarly, for the case $\mu \equiv -1$ and $p = \infty$ we have:

$$f^{k+1}(u) = f^k(u) - ||\big(\nabla_w^- f^k\big)(u)||_\infty, \tag{23}$$

which can be interpreted as an iteration of the following *nonlocal erosion* operator:

$$f^{k+1}(u) = \mathrm{NLE}\big(f^k\big)(u), \tag{24}$$

for which $\mathrm{NLE} : \mathcal{H}(V) \to \mathcal{H}(V)$ is defined as

$$\mathrm{NLE}\big(f\big)(u) = f(u) - \max_{u\sim v}\Big(\sqrt{w(u,v)}\big(f(v)-f(u)\big)^-\Big). \tag{25}$$

2.3 Our Previous Works on the p- and ∞-Laplacian on Graphs

In graph theory, there exist different expressions for the p-Laplacian on graphs [15,43]. In the context of PdEs on graphs (based on the weighted finite difference and divergence operators introduced above), we mimic the classical definition of the p-Laplacian on Euclidean domains to derive a unified form for two different expressions: the anisotropic and the isotropic graph p-Laplacian.

Anisotropic graph p-Laplacian The *anisotropic graph p-Laplacian* of a function $f \in \mathcal{H}(V)$, denoted by $\Delta^a_{w,p} : \mathcal{H}(V) \to \mathcal{H}(V)$, is defined as:

$$(\Delta^a_{w,p} f)(u) = \frac{1}{2} \operatorname{div}_w \Big(|(\mathcal{G}_w f)|^{p-2} (\mathcal{G}_w f) \Big)(u), \qquad (26)$$

for $1 \leq p < \infty$. Using (5) and (6), the anisotropic graph p-Laplace operator of $f \in \mathcal{H}(V)$ at a vertex $u \in V$ can be computed by [11,27]:

$$(\Delta^a_{w,p} f)(u) = \sum_{v \sim u} \sqrt{w(u,v)}^p |f(v) - f(u)|^{p-2}(f(v) - f(u)). \qquad (27)$$

Note that this operator can be seen as the discrete differential of the p-Dirichlet functional in (17).

If we use the notation:

$$\frac{\partial f}{\partial e}|_u = \partial_v f(u), \quad \text{with } e = (u, v), \qquad (28)$$

then the anisotropic graph p-Laplacian can be written as:

$$(\Delta^a_{w,p} f)(u) = \frac{1}{2} \sum_{\substack{e=(u,v) \\ v\sim u}} \frac{\partial}{\partial e} \left[\left| \frac{\partial f}{\partial e} \right|^{p-2} \frac{\partial f}{\partial e} \right] |_u. \qquad (29)$$

Remark 1 It gets clear that the anisotropic graph p-Laplacian in (27) can be seen as discrete analogue of the anisotropic p-Laplacian in the continuous case with $f : \Omega \subset \mathbb{R}^n \to \mathbb{R}$, defined as:

$$\Delta_p f(x) = \sum_{i=1}^{n} \frac{\partial}{\partial x_i} \left(\left| \frac{\partial f(x)}{\partial x_i} \right|^{p-2} \frac{\partial f(x)}{\partial x_i} \right), \qquad (30)$$

which can be seen as the differential of the continuous Dirichlet functional $\int_\Omega \sum_{i=1}^n \left| \frac{\partial f(x)}{\partial x_i} \right|^p \mathrm{d}x$.

Remark 2 Let us remark that the graph p-Laplacian can be interpreted as discrete version of the continuous nonlocal p-Laplacian. Indeed, we consider a complete Euclidean graph $G = (V, E, w)$, *i.e.,* $E = V \times V$, with $V = \Omega \subset \mathbb{R}^n$ and $f : \Omega \to \mathbb{R}$. Then, if we replace the sum in (27) by an integral, we obtain the nonlocal p-Laplacian [3]:

$$\mathcal{L}_p f(x) = \int_\Omega \mu(x, y, p)|f(y) - f(x)|^{p-2}(f(y) - f(x))\mathrm{d}y, \qquad (31)$$

with $\mu(x, y, p) = w(x, y)^{p/2}$. Note that in the continuous case $\mu \colon \mathbb{R}^n \to \mathbb{R}$ is a nonnegative continuous radial function with compact support and $\mu(0) > 0$ and $\int_{\mathbb{R}^n} \mu(x)\mathrm{d}x = 1$.

Isotropic graph p-Laplacian : The *isotropic graph p-Laplacian*, denoted by $\Delta^i_{w,p} : \mathcal{H}(V) \to \mathcal{H}(V)$, is defined as:

$$(\Delta^i_{w,p} f)(u) = \frac{1}{2} \operatorname{div}_w \Big(||\nabla_w f||_2^{p-2} (\mathcal{G}_w f) \Big)(u), \qquad (32)$$

with $1 \leq p < \infty$. Using the notation from above, this operator can be written fully as:

$$(\Delta^i_{w,p} f)(u) = \frac{1}{2} \sum_{\substack{e=(u,v) \\ v\sim u}} \frac{\partial}{\partial e} \left[||\nabla_w f||_2^{p-2} \frac{\partial f}{\partial e} \right] |_u. \qquad (33)$$

Using (5), (6), and (11), the isotropic graph p-Laplacian of $f \in \mathcal{H}(V)$ at a vertex $u \in V$ can be computed by

$$(\Delta^i_{w,p} f)(u) = \sum_{v \sim u} w(u, v)\big(||\nabla_w f(v)||_2^{p-2} - ||\nabla_w f(u)||_2^{p-2}\big)\big(f(v) - f(u)\big). \qquad (34)$$

For the case $p = 2$ and using either the isotropic or anisotropic Laplacian operator on graphs, we obtain a discrete variant of the classical (unnormalized) Laplacian:

$$(\Delta^u_{w,2} f)(u) = \sum_{v \sim u} w(u, v) \left(f(v) - f(u) \right). \qquad (35)$$

Similarly, using scalar products on $\mathcal{H}(V)$ (respectively, $\mathcal{H}(E)$) which depend on the degree of a vertex (respectively, the edge weight) we obtain the discrete normalized Laplacian on graphs as:

$$(\Delta_{w,2} f)(u) = \frac{\sum_{v \sim u} w(u, v) f(v)}{\delta_w(u)} - f(u). \qquad (36)$$

In the sequel, we will only consider the discrete normalized Laplacian operator in (36), which we will simply refer to as Laplacian.

All the above-introduced operators can be used to approximate continuous PDEs involving the p-Laplacian. In particular, if we consider the case $p = 2$ the equation

$$\frac{\partial f(x, t)}{\partial t} = \Delta f(x, t), \qquad (37)$$

can be approximated in a discrete setting as

$$\frac{\partial f(u, t)}{\partial t} = \Delta_{w,2} f(u, t). \qquad (38)$$

Employing a forward Euler time discretization with $\Delta t = 1$, an evolutionary process can be written as

$$f^{k+1}(u) = \mathrm{NLM}\big(f^k\big)(u), \qquad (39)$$

for which the operator NLM : $\mathcal{H}(V) \to \mathcal{H}(V)$ is the well-known nonlocal mean filter [14], defined as

$$\mathrm{NLM}(f) = \frac{\sum_{v \sim u} w(u,v) f(v)}{\delta_w(u)}. \tag{40}$$

∞-Laplacian : The nonlocal ∞-Laplacian of a function $f \in \mathcal{H}(V)$, denoted by $\Delta_{w,\infty} : \mathcal{H}(V) \to \mathcal{H}(V)$, is defined as [25]:

$$\Delta_{w,\infty} f(u) \stackrel{def.}{=} \frac{1}{2} \left[||(\nabla_w^+ f)(u)||_\infty - ||(\nabla_w^- f)(u)||_\infty \right], \tag{41}$$

which can be written fully as

$$\begin{aligned} \Delta_{w,\infty} f(u) = \frac{1}{2} \Big[&\max\Big(\sqrt{w(u,v)}\big(f(v) - f(u)\big)^+\Big) \\ &- \max\Big(\sqrt{w(u,v)}\big(f(v) - f(u)\big)^-\Big)\Big]. \end{aligned} \tag{42}$$

Remark As in the continuous case, this operator can be formally derived by the minimization of the following energy on graphs (for $p \to \infty$):

$$J_{w,p}(f) = \sum_{u \in V} ||\big(\nabla_w f\big)(u)||_p^p. \tag{43}$$

Indeed, it is easy to show [25] that the minimization of $J_{w,p}(f)$ leads to the PdE

$$\Delta_{w,p} f(u) = 0.$$

Normalized p-Laplacian : We shortly recall that the normalized version of the continuous p-Laplacian operator, referred to as game p-Laplacian, is defined [38] as

$$\Delta_p^N f(x) = \frac{1}{p|\nabla f(x)|^{p-2}} \Delta_p f(x). \tag{44}$$

This operator was recently introduced to discuss a stochastic game called Tug-of-war with noise [60]. It can be further rewritten as:

$$\Delta_p^N f = \frac{(p-2)}{p} \Delta_\infty^N f + \frac{1}{p} \Delta f = a \Delta_\infty^N f + b \Delta f, \tag{45}$$

with $a = (p-2)/p$ and $b = 1/p$. In the case $p = \infty$, we have:

$$\Delta_\infty^N f = \frac{1}{|\nabla f|^2} \Delta_\infty f. \tag{46}$$

A discrete version of this graph ∞-Laplacian has been introduced and investigated in [25]. Finally, the discrete normalized p-Laplacian operator of a function $f \in \mathcal{H}(V)$, denoted by $\Delta_{\alpha,\beta} : \mathcal{H}(V) \to \mathcal{H}(V)$, is defined as [26]:

$$\Delta_{\alpha,\beta} f = \frac{\alpha}{2} \big(||\nabla_w^+ f||_\infty - ||\nabla_w^- f||_\infty \big) + \beta \Delta_{w,2} f, \tag{47}$$

with $\alpha, \beta \geqslant 0$ and $\alpha + \beta = 1$.

3 A New Family of Graph p-Laplacian with Gradients Terms

In this section, we propose a new family of discrete operators on weighted graphs which corresponds to a graph p-Laplacian with gradients terms. Furthermore, we investigate an associated Dirichlet problem and study some connections between the latter, nonlocal continuous PDEs, and also a stochastic game known as Tug-of-War.

3.1 Definition

Based on the discussed PdE framework on graphs and the introduced approximations of the p-Laplacian and the ∞-Laplacian in Sect. 2, we are now able to propose a novel family of p-Laplacian operators denoted by $\Delta_{\alpha,\beta,\gamma} : \mathcal{H}(V) \to \mathcal{H}(V)$ for a function $f \in \mathcal{H}(V)$ by:

$$\Delta_{\alpha,\beta,\gamma} f \;=\; \alpha ||\nabla_w^+ f||_\infty - \beta ||\nabla_w^- f||_\infty + \gamma \Delta_{w,2} f, \tag{48}$$

for constants $\alpha, \beta, \gamma \geqslant 0$ and $\alpha + \beta + \gamma = 1$. By a simple factorization of the ∞-Laplacian, this new family of operators can be rewritten as:

$$\begin{aligned} \Delta_{\alpha,\beta,\gamma} f = &\,2\min(\alpha,\beta) \Delta_{w,\infty} f + (\alpha - \beta)^+ ||\nabla_w^+ f||_\infty \\ &- (\alpha - \beta)^- ||\nabla_w^- f||_\infty + \gamma \Delta_{w,2} f. \end{aligned} \tag{49}$$

As we demonstrate in the following, this formulation recovers many well-known expressions of the Laplacian, the ∞-Laplacian, and the p-Laplacian with gradients terms, depending on the choice of the three parameters α, β, and γ. First, we discuss the general case $\gamma \neq 0$:

- for $\gamma = 1$ and $\alpha = \beta = 0$, the expression (49) recovers the Laplacian operator:

$$\Delta_{\alpha,\beta,\gamma} f = \Delta_{w,2} f. \tag{50}$$

- for $\alpha = \beta \neq 0$, the expression (48) becomes:

$$\Delta_{\alpha,\beta,\gamma} f = \alpha \big(||\nabla_w^+ f||_\infty - ||\nabla_w^- f||_\infty \big) + \gamma \Delta_{w,2} f, \tag{51}$$

which is a discrete approximation of the continuous normalized p-Laplacian

$$\Delta_p^N f = 2\alpha \Delta_\infty^N f + \gamma \Delta f, \tag{52}$$

also recovering the discrete normalized p-Laplacian operator introduced in (47).

- for $\alpha - \beta > 0$, the expression (49) becomes:

$$\Delta_{\alpha,\beta,\gamma} f = (\alpha - \beta)||\nabla_w^+ f||_\infty + 2\beta\Delta_{w,\infty} f + \gamma\Delta_{w,2} f, \tag{53}$$

which is a discrete approximation of the continuous p-Laplacian with additional gradient terms:

$$\Delta_p f = (\alpha - \beta)||\nabla f|| + 2\beta\Delta_\infty f + \gamma\Delta f. \tag{54}$$

- for $\alpha - \beta < 0$, the expression (49) becomes:

$$\Delta_{\alpha,\beta,\gamma} f = (\alpha - \beta)||\nabla_w^- f||_\infty + 2\alpha\Delta_{w,\infty} f + \gamma\Delta_{w,2} f, \tag{55}$$

which is also a discrete approximation of the continuous p-Laplacian with additional gradient terms:

$$\Delta_p f = (\alpha - \beta)||\nabla f|| + 2\alpha\Delta_\infty f + \gamma\Delta f. \tag{56}$$

Next, we discuss the general case of $\gamma = 0$:

- for $\alpha > \beta$ one gets the following expression:

$$\Delta_{\alpha,\beta,\gamma} f = (\alpha - \beta)||\nabla_w^+ f||_\infty + 2\beta\Delta_{w,\infty} f, \tag{57}$$

- for $\alpha < \beta$ one gets the following expression:

$$\Delta_{\alpha,\beta,\gamma} f = (\alpha - \beta)||\nabla_w^- f||_\infty + 2\alpha\Delta_{w,\infty} f, \tag{58}$$

- for $\alpha = \beta$ the expression (49) recovers the ∞-Laplacian as:

$$\Delta_{\alpha,\beta,\gamma} f = \frac{1}{2}\big(||\nabla_w^+ f||_\infty - ||\nabla_w^- f||_\infty\big). \tag{59}$$

Note that this family of operators is directly related to the nonlocal average operator:

$$\Delta_{\alpha,\beta,\gamma} f = \mathrm{NLA}(f) - f, \tag{60}$$

for which we refer to the operator $\mathrm{NLA} : \mathcal{H}(V) \to \mathcal{H}(V)$ as 'nonlocal average' with

$$\mathrm{NLA}(f) = \alpha\mathrm{NLD}(f) + \beta\mathrm{NLE}(f) + \gamma\mathrm{NLM}(f), \tag{61}$$

and the operators NLD, NLE, and NLM as introduced in Sect. 2. Obviously, this family of operators can be expressed with the help of nonlocal mean, nonlocal erosion, and nonlocal dilation. In particular, for any unweighted graph with a constant weighting function $w \equiv 1$, we obtain the following expressions:

$$\begin{aligned} \mathrm{NLD}(f)(u) &= \max_{v \sim u} f(v), \\ \mathrm{NLE}(f)(u) &= \min_{v \sim u} f(v), \\ \mathrm{NLM}(f)(u) &= \frac{\sum_{v \sim u} f(v)}{|v \sim u|}. \end{aligned} \tag{62}$$

Thus, (61) can be rewritten as:

$$\mathrm{NLA}(f)(u) = \alpha \max_{v \sim u} f(v) + \beta \min_{v \sim u} f(v) + \frac{\sum_{v \sim u} f(v)}{|v \sim u|}. \tag{63}$$

3.2 Dirichlet Problem

In the following, we focus on a PdE related to the proposed family of graph p-Laplacian operators with gradient terms. In particular, we investigate an associated Dirichlet problem. Let $G = (V, E, w)$ be an undirected, weighted, and connected graph, $A \subset V$ a subset of vertices, and $g : \partial A \to \mathbb{R}$ a function defined on the boundary of A. We consider the PdE

$$\begin{cases} (\Delta_{\alpha,\beta,\gamma} f)(u) = 0, & u \in A, \\ f(u) = g(u), & u \in \partial A, \end{cases} \tag{64}$$

for the general case $\gamma \neq 0$. We demonstrate in the following that the problem (64) has a unique solution.

Theorem 1 *Given $G = (V, E, w)$, a set $A \subset V$, and a function $g : \partial A \to \mathbb{R}$, then there exists a unique function $f \in \mathcal{H}(V)$ such that f solves the following equation:*

$$\begin{cases} \alpha||\big(\nabla_w^+ f\big)(u)||_\infty - \beta||\big(\nabla_w^- f\big)(u)||_\infty \\ \qquad\qquad + \gamma(\Delta_{w,2} f)(u) = 0, & u \in A \\ f(u) = g(u), & u \in \partial A. \end{cases} \tag{65}$$

Proof First, we note that (65) can be rewritten as $f(u) = \mathrm{NLA}(f)(u)$. We begin by proving the uniqueness of the solution of (65) (if it exists) by using the comparison principle. We then prove its existence by using the Brouwer fixed point theorem.

Uniqueness Let f and h be two functions having the same values on ∂A and with $f = \mathrm{NLA}(f)$ and $h = \mathrm{NLA}(h)$ on A. Under these conditions, we can apply Lemma 2 on f and h, which leads to the fact that the inequality $f \leq h$ on ∂A can be extended to A. By exchanging the roles of f and h, we also obtain the opposite inequality and thus we can conclude that $f = h$ on A.

Existence First, let us recall the Brouwer fixed point theorem: A continuous function mapping from a convex, compact subset of a Euclidean space to the same set has a fixed point. We identify $\mathcal{H}(V)$ as $\mathbb{R}^n$ and consider the set $K = \{f \in \mathcal{H}(V) \mid f(u) = g(u)\ \forall u \in \partial A,\ \text{and}\ m \leqslant f(u) \leqslant M\ \forall u \in A\}$, for which $m = \min_{\partial A}\big(g(u)\big)$ and $M = \max_{\partial A}\big(g(u)\big)$. By definition, K is a convex and compact subset of $\mathbb{R}^n$. It is easy to show that the map $f \to \mathrm{NLA}\big(f\big)$ is continuous and maps from K into K. So, by application of the Brouwer fixed point theorem, the map NLA has a fixed point that is a solution of $\mathrm{NLA}\big(f\big) = f$. This completes the proof. □

Lemma 2 *Given two functions f and h, if $f = NLA(f)$ and $h = NLA(h)$ with $f \leq h$ on ∂A, then $f \leq h$ on the whole domain V.*

Proof We perform a proof by contradiction. Let us therefore expect that there exists $M \in \mathbb{R}$ such that

$$M = \sup_V (f - h) > 0.$$

Let $B = \{u \in A : f(u) - h(u) = M\}$, then by construction we have $B \neq \emptyset$ and $B \cap \partial A = \emptyset$. Now, we can claim that there exists a $u_0 \in B$ and $v \in N(u_0)$, such that $v \notin B$. Otherwise, if for each $u \in A$ and for each $v \in N(u)$ we have $v \notin B$, this would imply that $B \cap \partial A \neq \emptyset$ since the graph G is connected; however, this leads to a contradiction. Thus, from the definition of M we have

$$\begin{aligned} f(u_0) - h(u_0) &\geq f(u) - h(u) \quad \forall u \in N(u_0)\\ h(u) - h(u_0) &\geq f(u) - f(u_0) \quad \forall u \in N(u_0). \end{aligned}$$

In particular, we can write

$$h(v) - h(u_0) > f(v) - f(u_0).$$

Based on these inequalities and using the definitions of nonlocal morphological processes introduced in Sect. 2.2, i.e., dilation and erosion, we have

$$\begin{aligned} &\max_{u\sim u_0}\Big(\sqrt{w(u_0,u)}\max\big(h(u)-h(u_0),0\big)\Big)\\ &\geq \max_{u\sim u_0}\Big(\sqrt{w(u_0,u)}\max\big(f(u)-f(u_0),0\big)\Big)\\ &\mathrm{NLD}\big(h\big)(u_0) - h(u_0) \geq \mathrm{NLD}\big(f\big)(u_0) - f(u_0). \end{aligned} \tag{66}$$

Similarly, we get:

$$\begin{aligned} &\max_{u\sim u_0}\Big(-\sqrt{w(u_0,u)}\min\big(h(u)-h(u_0),0\big)\Big)\\ &\geq \max_{u\sim u_0}\Big(-\sqrt{w(u_0,u)}\min\big(f(u)-f(u_0),0\big)\Big)\\ &h(u_0) - \mathrm{NLE}\big(h\big)(u_0) \leq f(u_0) - \mathrm{NLE}\big(f\big)(u_0). \end{aligned} \tag{67}$$

Finally, we have

$$\begin{aligned} &\frac{\sum_{u\sim u_0} w(u_0,u)\big(h(u)-h(u_0)\big)}{\sum_{u\sim u_0} w(u_0,u)}\\ &> \frac{\sum_{u\sim u_0} w(u_0,u)\big(f(u)-f(u_0)\big)}{\sum_{u\sim u_0} w(u_0,u)}\\ &\mathrm{NLM}\big(h\big)(u_0) - h(u_0) > \mathrm{NLM}\big(f\big)(u_0) - f(u_0). \end{aligned} \tag{68}$$

Note that the previous inequality is strict because we know there exists a $v \in N(u_0)$ such that $h(v) - h(u_0) > f(v) - f(u_0)$.

Using (66), (67), and (68), we can deduce the following inequalities

$$\begin{aligned} &\alpha\mathrm{NLD}\big(h\big)(u_0) + \beta\mathrm{NLE}\big(h\big)(u_0) + \gamma\mathrm{NLM}\big(h\big)(u_0) - h(u_0)\\ &\alpha\mathrm{NLD}\big(f\big)(u_0) + \beta\mathrm{NLE}\big(f\big)(u_0) + \gamma\mathrm{NLM}\big(f\big)(u_0) - f(u_0). \end{aligned}$$

and

$$\begin{aligned} &\mathrm{NLA}\big(h\big)(u_0) - h(u_0) > \mathrm{NLA}\big(f\big)(u_0) - f(u_0)\\ &\quad\Rightarrow h(u_0) - h(u_0) > f(u_0) - f(u_0)\\ &\qquad\qquad \Rightarrow 0 > 0. \end{aligned}$$

This clearly leads to a contradiction and concludes the proof. □

3.3 Connection to Tug-of-War Games and Corresponding PDEs

Certain PDEs which involve a variant of the p-Laplace operator are related to a stochastic game called Tug-of-War, see e.g., [50,59] and references therein. In the following, we demonstrate that the proposed family of graph p-Laplacian operators recovers value functions for this game. In particular, we discuss the connection to conventional Tug-of-War games [59], the biased Tug-of-War game [58], and Tug-of-War games with noise [60].

Tug-of-War games Let us briefly review the notion of the stochastic Tug-of-War game as introduced by Peres, Schramm, Sheffield, and Wilson [59]. Let $\Omega \subset \mathbb{R}^n$ be an open, connected subset and $g : \partial\Omega \to \mathbb{R}$ a real function. Let $\varepsilon > 0$ be fixed. The dynamic of this two-player zero-sum game can be explained as follows: A token is placed at an initial position $x_0 \in \Omega$. At the kth stage of the game, Player I and Player II select two respective points x_k^I and x_k^{II} within a local ball $B_\varepsilon(x_{k-1}) \subseteq \Omega$ with radius ε centered in x_{k-1}. The game token is then moved to a new location x_k which is chosen as $x_k = x_k^I$ with probability $P = \frac{1}{2}$ or $x_k = x_k^{II}$ else. In other words, a fair coin is tossed to determine the new location of the game token. After the kth stage of the game, if $x_k \in \Omega$, the game continues to stage $k+1$. Otherwise, if $x_k \in \partial\Omega$, then the game ends and Player II pays Player I the amount $g(x_k)$ defined on the boundary of Ω. Hence, the dynamics of the Tug-of-War game lead to the fact that Player I attempts to maximize his payoff, while Player II attempts to minimize it.

According to the dynamic programming principle (DPP), the value functions for Player I and Player II for the above-described conventional ε-turn Tug-of-War game satisfy the relation

$$\begin{cases} f^\varepsilon(x) = \frac{1}{2}\left[\max_{y\in B_\varepsilon(x)} f^\varepsilon(y) + \min_{y\in B_\varepsilon(x)} f^\varepsilon(y)\right], & x\in\Omega \\ f^\varepsilon(x) = g(x), & x\in\partial\Omega. \end{cases} \tag{69}$$

In [59], the authors show that for $\epsilon \to 0$, one has $f^\epsilon \to f$ in a certain sense, for which f is a solution of the ∞-Laplacian equation:

$$\begin{cases} \Delta_\infty f(x) = 0, & x\in\Omega \\ f(x) = g(x), & x\in\partial\Omega. \end{cases} \tag{70}$$

Now, let us investigate the Euclidean graph $G=(V,E,w)$ with $V=\Omega\subset\mathbb{R}^n$, $E=\{(x,y)\in V\times V \mid w(x,y)>0\}$, and

$$w(x,y) = \begin{cases} 1, & \text{if } |y-x| \leqslant \varepsilon, \\ 0 & \text{otherwise.} \end{cases} \tag{71}$$

We use the following relations, which can be easily obtained from the definitions of the $\mathcal{L}_\infty$ norms of morphological gradients in (14)

$$\max_{y\in B_\varepsilon(x)} f(y) = ||\big(\nabla_w^+ f\big)(x)||_\infty + f(x),$$
$$\min_{y\in B_\varepsilon(x)} f(y) = f(x) - ||\big(\nabla_w^- f\big)(x)||_\infty.$$

By replacing the max and min functions in (69) by their respective discrete gradient variants, we get:

$$\frac{1}{2}\left(||(\nabla_w^+ f)(x)||_\infty - ||(\nabla_w^- f)(x)||\right) = 0. \tag{72}$$

It gets clear that in the case $\gamma = 0$ and $\alpha = \beta = 0.5$ our formulation (48), which in this case represents the ∞-Laplacian on graphs, coincides with the value function (69) of the conventional Tug-of-War game.

Biased Tug-of-War games Now, we concentrate on another variant of the conventional Tug-of-War game. To obtain the biased Tug-of-War game, the above variant is modified as follows [58]: One considers two fixed real numbers $\alpha, \beta > 0$ with $\alpha+\beta = 1$. The biased Tug-of-War game follows the same game dynamics as described above with the only difference that the probability of the next location is set for x_k^I as α and for x_k^{II} as β.

According to the DPP, the value function in this case becomes [58]:

$$\begin{cases} f^\varepsilon(x) = \alpha \max_{y\in B_\varepsilon(x)} f^\varepsilon(y) + \beta \min_{y\in B_\varepsilon(x)} f^\varepsilon(y), & x\in\Omega \\ f^\varepsilon(x) = g(x), & x\in\partial\Omega. \end{cases} \tag{73}$$

When $\varepsilon \to 0$, the solution converges to the ∞-Laplacian equation with gradient terms:

$$\Delta_\infty f(x) + c||(\nabla f)(x)|| = 0, \tag{74}$$

and c which depends on α and β [58].

Analogously, by replacing the min and max functions in (73) by their respective discretized gradient versions we get:

$$\alpha||(\nabla_w^+ f)(x)||_\infty - \beta||(\nabla_w^- f)(x)||_\infty = 0, \tag{75}$$

which can be written in terms of the proposed family of operators as $\Delta_{\alpha,\beta,\gamma} = 0$ for $\alpha > 0$, $\beta > 0$, and $\gamma = 0$.

Tug-of-War game with noise This game also follows the same game dynamics as the classical Tug-of-War game. However, here the probability to have the token location to be x_k^I or x_k^{II} is $\frac{\alpha}{2}$, while with probability $\frac{\beta}{2}$ the next location is chosen as a random point in the ball $B_\varepsilon(x)$. The authors of [50] have shown that the value functions of this game satisfy the DPP and can be given as

$$\begin{aligned} f^\varepsilon(x) &= \frac{\alpha}{2}\left[\max_{y\in B_\varepsilon(x)} f^\varepsilon(y) + \min_{y\in B_\varepsilon(x)} f^\varepsilon(y)\right] \\ &\quad + \frac{\beta}{|B_\varepsilon(x)|}\int_{B_\varepsilon(x)} f^\varepsilon(y)\mathrm{d}y, \quad x\in\Omega, \\ f^\varepsilon(x) &= g(x), \qquad x\in\partial\Omega \end{aligned} \tag{76}$$

and $\alpha, \beta > 0$ such that $\alpha+\beta = 1$.

The authors of [60] show that when $\varepsilon \to 0$, $f^\varepsilon(x) \to f(x)$ and the solution of (76) converges to the solution of $\Delta_p f(x) = 0$ with $p > 2$, defined as:

$$\begin{cases} \Delta_p f(x) = \operatorname{div}(||\nabla f(x)||^{p-2}\cdot\nabla f(x)) = 0, & x\in\Omega \\ f(x) = g(x), & x\in\partial\Omega, \end{cases} \tag{77}$$

Analogously, by replacing the min and max functions in (76) by their respective discretized gradient versions, and using $\alpha = \beta$ and $\gamma \neq 0$, we can rewrite (76) as:

$$\alpha\left[||(\nabla_w^+ f)(x)||_\infty + ||(\nabla_w^- f)(x)||_\infty\right] + \gamma(\Delta_{w,2} f)(x) = 0 \tag{78}$$

Now if we consider the same Euclidean graph G, the solution of the following equation:

$$\Delta_{\alpha,\beta,\gamma} f^\varepsilon(x) = 0, \tag{79}$$

corresponds to the following DPP:

$$\begin{aligned} f^\varepsilon(x) = \alpha \max_{y\in B_\varepsilon(x)} f^\varepsilon(y) + \beta \min_{y\in B_\varepsilon(x)} f^\varepsilon(y) \\ + \frac{\gamma}{|B_\varepsilon(x)|}\int_{B_\varepsilon(x)} f(y)^\varepsilon \mathrm{d}y \text{ on } \Omega, \end{aligned} \tag{80}$$

This DPP corresponds to the biased Tug-of-War with noise, with the difference that the probability for x_k^I being the next location is α, while being x_k^{II} is β, and for a random point is γ.

Nonlocal Tug-of-War In this section, we demonstrate that the proposed graph p-Laplacian operator with gradient terms corresponds to a nonlocal Tug-of-War game. We have shown that for particular local Euclidean graphs this formulation corresponds to many known Tug-of-War games. Now if we consider general weighted graphs, we show that our formulation corresponds to nonlocal Tug-of-War games. For the sake of brevity, we only illustrate this observation for the case $\alpha = \beta = \frac{1}{2}$, and $\gamma = 0$, but the same interpretation still holds for general α, β and γ values.

If we consider a complete weighted graph $G = (V, E, w)$ for $\alpha = \beta = \frac{1}{2}$, $\gamma = 0$, and $u \in N(u)$, then we have:

$$\begin{aligned} \Delta_{\alpha,\beta,\gamma} f(u) &= ||(\nabla_w^+ f)(u)||_\infty - ||(\nabla_w^- f)(u)||_\infty \\ &= \max_{v\in V}\left(\sqrt{w(u,v)}(f(v) - f(u))\right) \\ &\quad + \min_{v\in V}\left(\sqrt{w(u,v)}(f(v) - f(u))\right) = 0. \end{aligned} \tag{81}$$

One can show that this equation is equivalent to the following condition:

$$\begin{aligned} f(u) = \max_{y\in V}\Bigg(\min_{z\in V}\Bigg(\frac{\sqrt{w(u,y)}}{\sqrt{w(u,y)}+\sqrt{w(u,z)}} f(y) \\ + \frac{\sqrt{w(u,z)}}{\sqrt{w(u,y)}+\sqrt{w(u,z)}} f(z)\Bigg)\Bigg). \end{aligned} \tag{82}$$

If one sets now

$$P(u,y,z) = \frac{\sqrt{w(u,y)}}{\sqrt{w(u,y)}+\sqrt{w(u,z)}}, \tag{83}$$

we can write:

$$\begin{aligned} f(u) = \max_{y\in V}\Big(\min_{z\in V}(P(u,y,z)f(y) \\ + (1 - P(u,y,z))f(z))\Big). \end{aligned} \tag{84}$$

This relationship can be interpreted as a nonlocal Tug-of-War game due to the generality of the weight function w.

For a general weighted Euclidean graph and setting $\gamma = 0$ and $\alpha = \beta = 0.5$, the proposed graph p-Laplacian is connected to a Tug-of-War game that can be interpreted as being nonlocal. The game dynamics for this novel stochastic game are the same as described above except that the ε-ball is replaced by a (possibly) nonlocal neighborhood $N(x_{k-1}) \subset \Omega$, given as

$$N(x_{k-1}) = \{x \in \Omega \mid w(x, x_{k-1}) > 0\}. \tag{85}$$

For this variant, the token at the kth stage of the game is moved to a new destination $x_k \in \Omega$, chosen randomly such that $x_k = x_k^I$ with a probability

$$P = \frac{\sqrt{w(x_{k-1}, x_k^I)}}{\sqrt{w(x_{k-1}, x_k^I)} + \sqrt{w(x_{k-1}, x_k^{II})}}, \tag{86}$$

and $x_k = x_k^{II}$ with a probability $1 - P$.

Using the relations in (83) and (84), this leads exactly to

$$\Delta_{\infty,w} f(x) = 0. \tag{87}$$

3.4 Connection to Continuous Nonlocal PDEs

We now discuss the relationship of the proposed family of graph operators with certain continuous nonlocal PDEs. Let $G = (V, E, w)$ be a Euclidean graph with $V = \Omega \subset \mathbb{R}^n$, $E = \{(x, y) \in V \times V \mid w(x, y) > 0\}$, and

$$w(x,y) = \begin{cases} \frac{1}{|x-y|^{2s}} & x \neq y,\ s \in [0,1] \\ 0 & \text{otherwise.} \end{cases} \tag{88}$$

In the case $\gamma = 0$ and $\alpha = \beta \neq 0$, it gets clear that the proposed family of graph p-Laplacian in (48) corresponds to the Hölder ∞-Laplacian equation, recently proposed by Chambolle et al. in [16], which is given as

$$\begin{aligned} \Delta_{w,\infty} f(x) = \frac{1}{2}\Bigg[\max_{y\in\Omega, y\neq x}\left(\frac{f(y) - f(x)}{|y-x|^s}\right) \\ + \min_{y\in\Omega, y\neq x}\left(\frac{f(y) - f(x)}{|y-x|^s}\right)\Bigg]. \end{aligned} \tag{89}$$

This operator is formally derived from the minimization of the following energy functional

$$\int_\Omega \int_\Omega \frac{[f(y) - f(x)|^p}{|x-y|^{p\times s}} \mathrm{d}x\mathrm{d}y \tag{90}$$

with $p \to \infty$.

In [16], the authors show that the equation

$$\begin{cases} \Delta_{w,\infty} f(u) = 0, & u \in \Omega \\ f(u) = g(u), & u \in \partial\Omega, \end{cases} \tag{91}$$

has a unique solution assuming some mild conditions on g.

For the case $\alpha = \beta = 0$, it gets clear that this formulation recovers the continuous nonlocal p-Laplacian equation given as

$$\int_\Omega w(x,y)\big(f(y) - f(x)\big)\mathrm{d}y = 0. \tag{92}$$

This operator has been recently used in many applications including continuum mechanics, population dynamics, and many different nonlocal diffusion problems [4]. One particular special case is given by

$$w(x,y) = \begin{cases} \frac{1}{|y-x|^{n+2s}}, & x \neq y, s \in [0,1], \\ 0, & \text{otherwise}. \end{cases} \tag{93}$$

Here, one recovers the continuous fractional Laplacian, which is commonly used to model anomalous diffusion:

$$(-\Delta)^s f(x) = C_{n,s} \int_{\mathbb{R}^n} \frac{f(y) - f(x)}{|y-x|^{n+2s}} \tag{94}$$

with a normalization factor $C_{n,s}$.

Finally, we underline that in the most general case (with arbitrary α, β, γ, and w), the proposed family of nonlocal graph p-Laplacian in (48) corresponds to PdEs which interpolate between the ∞-Laplacian, the Laplacian, and gradient terms.

4 Unified Interpolation for Inverse Problems on Images and Point Clouds

In this section, we illustrate the behavior of the proposed family of graph p-Laplace operators with gradient terms by using it to solve several selected inverse problems, which correspond to restoration or interpolation problems on graphs.

Many tasks in computer vision and image processing can be formulated as interpolation problems. Image and video colorization [46], inpainting [5,63], and semi-supervised segmentation [33,74] are examples of these interpolation problems. In general, interpolation consists of estimating appropriate values in regions of missing data while staying coherent with respect to the given data. Until today, many methods have been developed and proposed for image interpolation [14,27,34,68]. Among them, a significant amount of methods is based on local or nonlocal PDEs or variational methods.

In this work, we propose to use the family of graph p-Laplace operators introduced in Sect. 3, as a unified framework. Among other tasks, this framework can be used to solve semi-supervised segmentation or clustering, image inpainting, as well as colorization of point clouds. To perform this task, we propose to solve the discussed Dirichlet problem from (64):

$$\begin{cases} \Delta_{\alpha,\beta,\gamma}\big(f\big)(u) = 0, & u \in A, \\ f(u) = g(u), & u \in \partial A, \end{cases} \tag{95}$$

for which $A \subset V$ is the subset of vertices associated with the missing information. Note that the initial value function g is application dependent and will be defined for each application in the sequel.

To solve (95), we make use of the following associated evolution equation problem:

$$\begin{cases} \frac{\partial}{\partial t} f(u,t) = \Delta_{\alpha,\beta,\gamma} f(u,t), & u \in A, \\ f(u,t) = g(u), & u \in \partial A, \\ f(u, t=0) = f_0(u), & u \in A, \end{cases} \tag{96}$$

for which f_0 is an initial function that is also application dependent.

To solve (96) iteratively we use an explicit forward Euler time discretization:

$$\frac{\partial f}{\partial t}(u,t) = \frac{f^{n+1}(u) - f^n(u)}{\Delta t} \tag{97}$$

with $f^n(u) = f(u, n\Delta t)$.

Hence, we can try to solve (96) by the following iteration scheme:

$$\begin{cases} f^{n+1}(u) = f^n(u) + \Delta t \Delta_{\alpha,\beta,\gamma} f^n(u), & u \in A, \\ f^{n+1}(u) = g(u), & u \in \partial A, \\ f^0(u) = f_0(u), & u \in A. \end{cases} \tag{98}$$

Using $\Delta_{\alpha,\beta,\gamma} = \mathrm{NLA}(f) - f$ and setting $\Delta t = 1$, we get the following nonlocal average filter, which is a convex combination of a dilation, an erosion, and a nonlocal mean process:

$$\begin{cases} f^{n+1}(u) = \alpha \text{NLD}(f^n)(u) + \beta \text{NLE}(f^n)(u) \\ \qquad\qquad + \gamma \text{NLM}(f^n)(u), & u \in A, \\ f^{n+1}(u) = g(u), & u \in \partial A, \\ f^0(u) = f_0(u), & u \in A. \end{cases} \tag{99}$$

4.1 Graph Construction

In order to apply the deduced iteration scheme in (99), we first have to discuss how to construct a particular graph for given data. In general, there exist several popular methods to transform any discrete data into a weighted graph structure. Considering a set of vertices V such that the data are described by functions of $\mathcal{H}(V)$, the construction of such a graph consists in modeling the neighborhood relationships between the data through the definition of a set of edges E and using a pairwise distance measure $\mu : V \times V \to \mathbb{R}^+$. In the particular case of images, edges based on geometric neighborhoods are particularly well adapted to represent the geometry. Typically, one constructs one of the following graphs :

- The *grid graph* is one of the most natural structures to describe an image by a graph. Each pixel is connected by an edge to its adjacent neighbors. Classical grid graphs are 4-adjacency grid graphs and 8-adjacency grid graphs. Larger neighborhoods can be used to obtain nonlocal graphs.
- The *k-neighborhood graph* (k-NNG), for which each vertex u is connected with its k-nearest neighbors with respect to a distance measure μ. Such construction implies to build a directed graph, since this neighborhood relationship is not symmetric. Nevertheless, an undirected graph can be obtained by adding an edge between two vertices u and v if u is among the k-nearest neighbors of v or if v is among the k-nearest neighbors of u. Note that this is the most straightforward structure to describe a point cloud with a graph, e.g., see [6].

The similarity between two vertices is computed by a similarity measure $s : E \to \mathbb{R}^+$, which satisfies :

$$w(u, v) = \begin{cases} s(u, v), & \text{if } (u, v) \in E \\ 0, & \text{otherwise} \end{cases}$$

Common similarity functions are the following :

$$s_0(u, v) \equiv 1,$$
$$s_1(u, v) = \exp\Big(-\mu\big(f^0(u), f^0(v)\big)/\sigma^2\Big),$$

for which the variance parameter $\sigma > 0$ usually depends on the variation of the function μ.

The function f used to describe the data at a node u can be considered as a feature vector. Several choices can be considered for the expression of the feature vectors, depending on the nature of the features to be used for graph processing. In the context of image processing, one can use a simple grayscale or color feature vector F_u, or a patch feature vector $F_u^\tau = \bigcup_{v \in \mathcal{W}^\tau(u)} F_v$ (i.e., the set of values F_v for which v is in a square window $\mathcal{W}^\tau(u)$ of size $(2\tau + 1) \times (2\tau + 1)$ centered at a vertex pixel u). Note that the latter vector allows to incorporate nonlocal features for $\tau \geq 1$.

Patch construction for 3D point clouds Extending the notion of a patch to three-dimensional point cloud data is not an easy task. In [49], we have proposed a novel definition of patches that can be used for any graph representation associated with meshes or point clouds. In particular, around each vertex we build a two-dimensional grid (the patch) describing the close neighborhood. This grid is defined on the tangent plane of the point (i.e., the vertex). Then the patch is oriented accordingly, and finally the patch is filled in with a weighted average of the graph signal values in the local neighborhood. The first step consists in estimating the orientation of each patch. The second step consists in the actual patch construction. The set of values inside the patch of the vertex u are denoted as $\mathcal{P}(u)$. Let $C_k(u)$ denote the kth cell of the constructed patch around u with $k \in \{1, \ldots, n^2\}$. With the proposed patch construction process, one can define the set $V_k(u) = \{v \mid \mathbf{p}'_v \in C_k(u)\}$ as the set of vertices v that was assigned to the kth patch cell of u. Then, the patch vector is defined as $\mathcal{P}(u) = \left(\frac{\sum_{v \in V_k(u)} w(\mathbf{c}_k, \mathbf{p}_v) f^0(v)}{\sum_{v \in V_k(u)} w(\mathbf{c}_k, \mathbf{p}_v)} \right)^T_{k \in \{1, \ldots, n^2\}}$ with $w(\mathbf{c}_k, \mathbf{p}_u) = \exp(-\frac{\|\mathbf{c}_k - \mathbf{p}'_u\|_2^2}{\sigma^2})$, for which $\mathbf{c_k}$ are the coordinates' vectors of the kth patch cell center. This weighting enables us to take into account the point distribution within the patch cells in order to compute their mean feature vectors. The Fig. 1a shows our patch construction method. Figure 1b, c demonstrates that points with similar geometric configurations are similar with respect to the patch distance.

4.2 3D Colorization

Image colorization is the process of adding colors to monochromatic images. Since color images are often much more appealing than their grayscale versions, colorization has attracted interest, especially in the movie industry. Early attempts were made by coloring each frame of a movie by hand. It gets easily clear that a manual colorization process is tedious, is time-consuming, and requires artistic skills to precisely add the appropriate colors to the image. Therefore, computer-aided colorization has been firstly introduced

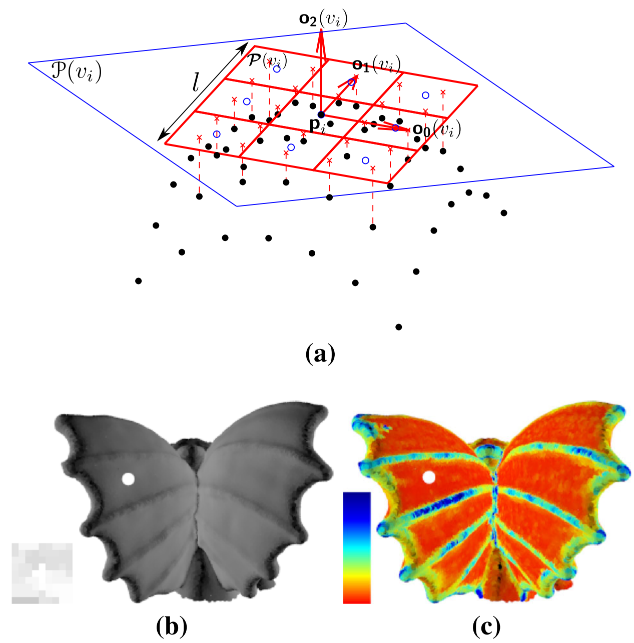

Fig. 1 **a** The interpolation of the content of the patch with a patch length of $l > 0$. $\mathbf{o}_0(u)$ and $\mathbf{o}_1(u)$ are the orientation of the patch $\mathcal{P}(u)$ at a point $\mathbf{p}_u$. Elements marked by a "times" symbol correspond to the projected neighbors $\mathbf{p}'_u$ of the point $\mathbf{p}_u$ on the patch. These projections are used to deduce values of each patch cell (a "o" symbol) by a weighted average of the associated graph signal values. **b** A point cloud with a selected vertex (in *white*) and the respective patch descriptor of that vertex. **c** A point cloud *colored* by the patch-based distance between all points and a selected one from most similar (in *red*) to least similar (in *blue*) (Color figure online)

by Markle [52]. One of the first computer-aided colorization processes has been used for the colorization of the Casablanca monochrome film in the 1980s. Since then, many movies have been converted into color versions and colorization processes have naturally received a lot of attention in the image-editing community. In recent years, many interactive colorization techniques have been proposed to effectively colorize images with significantly reduced amount of user efforts. Most of these techniques are based on color input examples (named color scribbles) given by a user, which are then propagated over the whole image. For instance, the method by Levin et al. [46] uses strokes to indicate colors for certain pixel regions. The whole image is then colorized using an optimization method which is based on intensity-continuity constraints, assuming adjacent pixels with similar intensities have similar colors. For recent techniques, see, e.g., [39,66,72] and references therein.

Recently, there has been a strong development of 3D acquisition techniques. This has led to a widespread acquisition of large amounts of 3D data and has brought point clouds to the forefront for a number of applications [54,61,62], and consequently, 3D point cloud data are now a new central data type in computer vision and graphics. However, many point clouds are colorless and, as for images, it might be desirable to add color information to 3D point clouds to add more realism to the scene. As pointed out in [44], this is of particular interest for cultural heritage applications where one wants to represent objects, e.g., statues, as colorful as they were at the time point of their creation.

Extending the colorization process to 3D data, such as meshes or point clouds, is not an easy task. Indeed, to colorize monochrome images the luminance channel is used to determine pixels similarities which enable color diffusion from scribbles. In the case of 3D data, however, the intensity channel is missing and similarities between points have to be determined in a different way. To the best of our knowledge, Leifman and Tal [44] are the only researchers which have proposed a method for *mesh colorization* up to now. Their central idea is to define similarities between mesh vertices using the spin image descriptor [37] together with a feature line detection. The colorization is then performed by solving a constrained quadratic optimization problem (as in [46]). They have further extended this work by pattern classification to reduce the set of color scribbles [45].

In the seminal work of Leifman and Tal [44], the authors have shown that extending the process of image colorization to 3D meshes is possible, but they do not consider the most recent type of 3D data nowadays available: 3D point clouds. As extending colorization to meshes is difficult, this is even more the case for 3D points clouds. Indeed, this type of data is very different to classical data structures used in computer graphics, e.g., triangulated meshes. In the case of 3D point clouds, the data take the form of unstructured raw point samples without any additional geometry. Since often a tremendous amount of 3D points is captured by a 3D acquisition device, no explicit mesh structure is required. This has the advantage that the high density of 3D point clouds enables to capture an object accurately without the need to model it. Moreover, for many applications it is important for conservation purposes to directly consider the raw point cloud and not a post-processed mesh because the process of mesh sampling generally leads to a loss of accuracy and details. Therefore, it is highly desirable to use methods which perform colorization of *raw 3D point clouds* directly. Unfortunately, since 3D points clouds have no intrinsic connectivity, it is very challenging to formulate a variational algorithm for 3D point cloud colorization, since the definition of basic differential operators on meshes have specific connectivity requirements which are only available for triangular meshes. As a consequence, the state-of-the-art methods proposed by Leifman and Tal in [44] for mesh colorization cannot be directly adapted to raw 3D point clouds. In the context of this work, we propose to interpret colorization as a particular color interpolation problem, for which the color information is the missing data.

In the following, we assume that the given data are defined on a general domain represented on a graph $G = (V, E, w)$.

Fig. 2 Comparison of the colorization results of [44] (*first row*) with the one of our approaches (*second row*). Our method considers directly the raw point cloud and does not require any preprocessing, whereas method of [44] processed by resampling and re-meshing input data before *colorization* step (Color figure online)

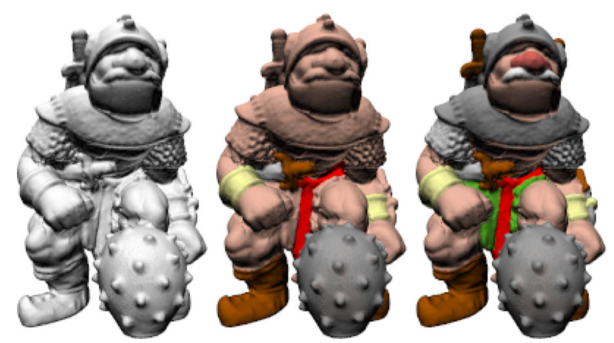

Fig. 3 From *left* to *right*: *uncolored* dwarf, *half-colored* dwarf, *fully colored* dwarf (Color figure online)

Let $f^0 : V \to \mathbb{R}^3$ be a function that assigns RGB colors to vertices. Let $A \subset V$ be the subset of vertices with unknown colors and ∂A the subset of vertices for which $g : \partial A \to \mathbb{R}^3$ gives the user-specified color scribbles. Then, we are able to use the unified framework proposed in Sect. 4 and, in particular, the iteration scheme (99) to perform 3D colorization of point cloud data.

Figure 3 shows exemplary results of 3D point cloud colorization of a dwarf figurine. We also compared our work with the state-of-the-art method [44]. The results of this comparison are presented in Fig. 2. The major drawback of [44] is the restricted applicability of this method to meshes only. For our proposed method, we have only considered the connection points of the mesh while discarding all given mesh connectivity information. As shown, e.g., in the third column of Fig. 2, our approach needs less color strokes, and we obtain much less color bleeding effects. Note that the proposed method in [44] also requires mesh preprocessing, such as resampling and re-meshing (see the vasis example in the last column of Fig. 2), whereas our method can be applied directly on the raw point cloud data. Figure 4 shows another example of colorization on a 3D point cloud, representing a bas-relief.

4.3 Nonlocal Inpainting

Digital inpainting is a fundamental problem in modern image processing and has many applications in different fields. This task can be simply formulated as reconstructing a damaged or incomplete image by filling the missing information in certain regions. In recent years, many methods have been developed for interpolating geometry [8,17], texture [21,24], or both geometry and texture [5,31]. Among the proposed interpolation methods, a significant number of algorithms are based on PDEs or variational methods, see, e.g., [5,63] and references therein. Since the seminal work of Buades et al.

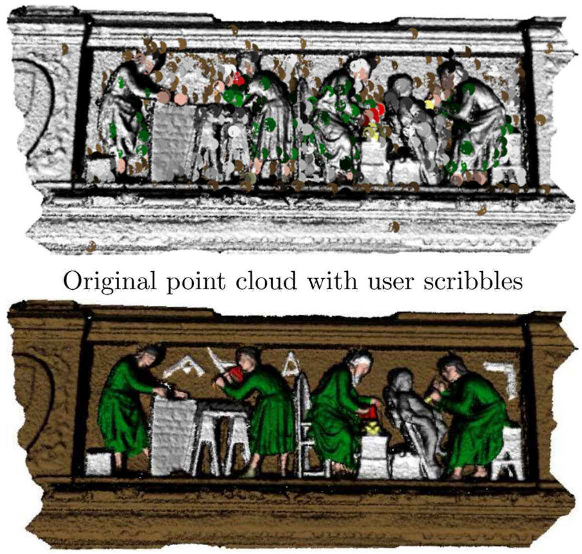

Fig. 4 *Colorization* of a scanned bas-relief (Color figure online)

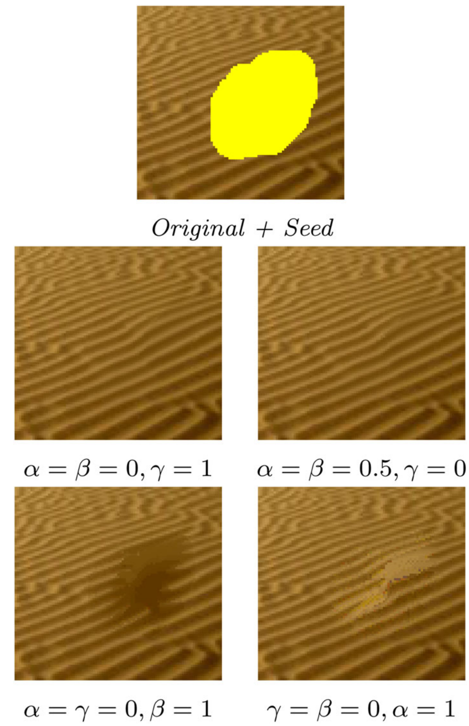

Fig. 5 Illustration of image inpainting using a nonlocal graph. Results have been computed using different values of the parameters α, β, and γ. See text for more details

on nonlocal filtering [14], many nonlocal methods for image inpainting have gained considerable attention. This is in part due to their superior performance for textured images, which is a known weakness of purely local methods. Recent works tend to unify local and nonlocal interpolation approaches [33]. A variational framework for nonlocal image inpainting has been presented in [5]. A discrete nonlocal regularization framework for image and manifold processing has been proposed in [32]. This framework has been used to unify local geometric methods and nonlocal exemplar-based methods for video inpainting.

With respect to (95), we propose to formulate the inpainting problem as follows: A is the set of pixels with missing information, $g : \partial A \to \mathbb{R}^c$ represents the known information (for which c is the number of color channels of the image), and $f : A \to \mathbb{R}^c$ represents the image to be reconstructed. Using this notation, we are able to use the iteration scheme (99) to perform nonlocal inpainting.

We illustrate this approach in Fig. 5 for different values of the parameters α, β, γ: $\alpha = \beta = 0, \gamma = 1$ corresponding to $\Delta_{w,2}$; $\alpha = \beta = 0.5, \gamma = 0$ corresponding to $\Delta_{w,\infty}$; $\alpha = \gamma = 0, \beta = 1$ corresponding to an erosion process; and $\gamma = \beta = 0, \alpha = 1$ corresponding to a dilation process. In this example, the constructed graph is a nonlocal grid graph built by using a 11×11 neighborhood window and 5×5 patches with a data-dependent weight function as discussed above in the case of point cloud data.

Figure 6 presents another application of graph inpainting for a texture reconstruction on colored 3D point cloud data. Following the idea presented in [48], the graph is built as a nonlocal k-NNG graph and the function f to be interpolated is associated with a color vector at each vertex of the graph. Applying again the unified framework proposed in Sect. 4, we are able to show results for different values of the parameters α, β, γ in Fig. 6, which correspond to $\Delta_{w,\infty}$, $\Delta_{w,2}$, a dilation process, and an erosion process, respectively. Figure 4 shows the inpainting on images on point clouds representing degraded antique objects. Figure 8 presents both geometric and image inpainting on a spherical point cloud.

4.4 Semi-supervised Segmentation and Classification

In the case of semi-supervised image segmentation, graph-based approaches have become very popular in recent years and many graph-based algorithms have been proposed, e.g., graph-cuts [12], random walkers [35], shortest path methods [7,30], watershed algorithms [10,20,70], or frameworks that unify some of the previous methods, such as power-watershed [19,65]. Recently, these algorithms have been embedded into a common general framework [19], which allows them to be interpreted as special cases. Several popular graph clustering approaches [7,20,22,30,53] consist in computing a graph partition from a set of user-defined seeds and a specified metric. For further details, we refer the interested reader to [22] (Figs. 7, 8).

In the context of this work, we propose to consider the semi-supervised segmentation task as an interpolation prob-

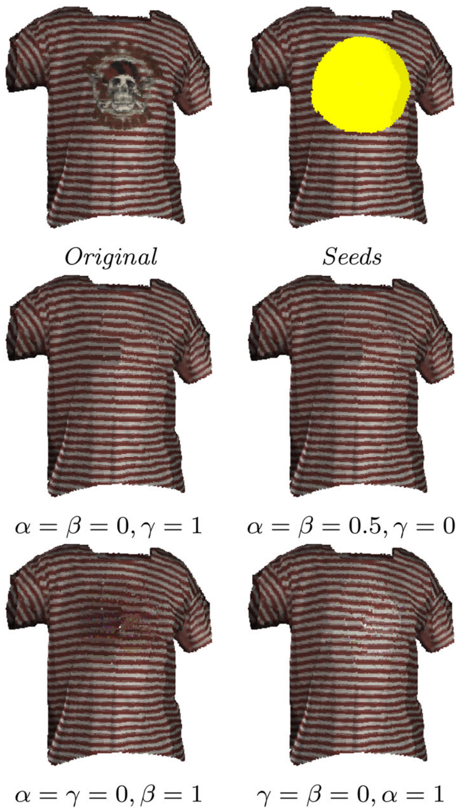

Fig. 6 Illustration of texture inpainting on a colored 3D point cloud using a nonlocal graph for different values of the parameters α, β, and γ. See text for more details

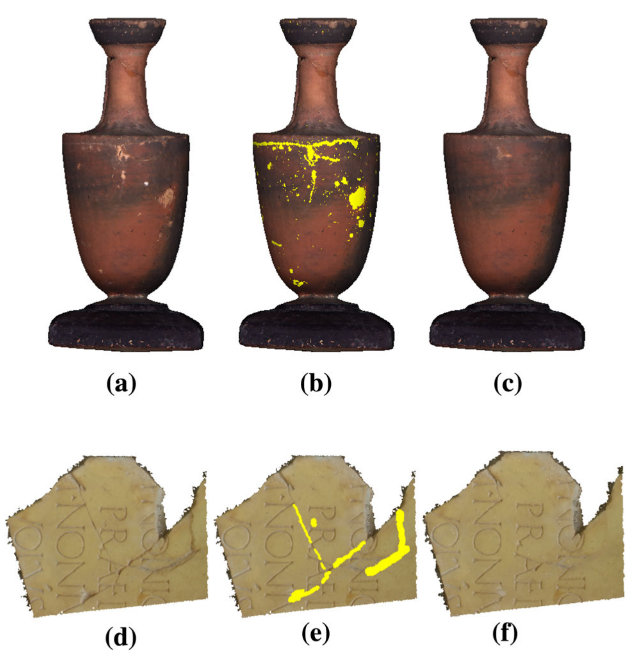

Fig. 7 Restoration of antique objects. **a** Original vasis, **b** vasis to inpaint, **c** restored vasis, **d** original wall, **e** wall to inpaint, **f** restored wall

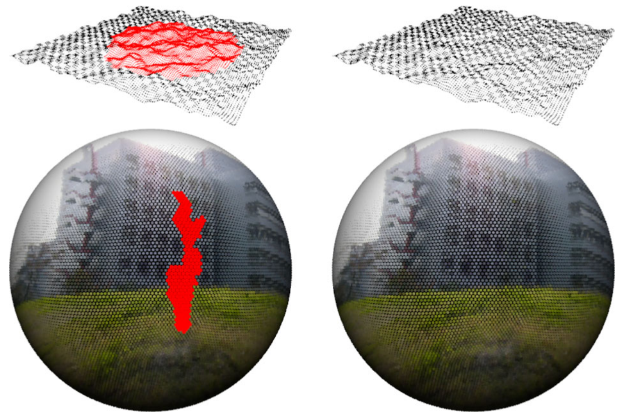

Fig. 8 Inpainting on a spherical point cloud

lem, for which the function to be interpolated is the label function specifying the partition. Using (95) and considering a partition into two classes A and B, the initial label function g is defined as follows

$$\begin{cases} g(u) = -1 & \text{if } u \in A \\ g(u) = 1 & \text{if } u \in B \\ g(u) = 0 & \text{otherwise} \end{cases} \tag{100}$$

After convergence to a solution f of (95), the class membership can be easily computed by simply thresholding the sign of f.

Remark In the case of $N > 2$ classes, a multiphase segmentation can be performed by applying the iteration scheme (95) N times and considering the label A as a class and B as the other classes. In this case, the label function L, associating a class with each vertex, defined as $L : V \to \{C_i\}_{i=1,\dots,N}$ with $\{C_i\}$ the set of class labels, is computed as:

$$L(u) = C_i \,|\, f_i(u) = \max_{j=1,\dots,N} f_j(u).$$

Real data clustering In this paragraph, we present some experiments for label diffusion based on the proposed family of graph p-Laplace operators $\Delta_{\alpha,\beta,\gamma}$ for the task of semi-supervised clustering. For testing, we use three standard databases from the literature which are composed of handwritten digits: MNIST [42], OPTDIGITS [2], and PENDIGITS [1]. For our experiments, we have merged both the training and the test data set (as also performed in [13]), resulting in data sets with 70,000, 5620, and 10,992 objects for MNIST, OPTDIGITS, and PENDIGITS, respectively.

For the task of semi-supervised classification, we consider each object of the database as a node of a graph and each object of the database is represented by a feature vector. To build a graph on these databases, we use the k-NNG graph construction described in Sect. 4.1 with $k = 10$ as performed

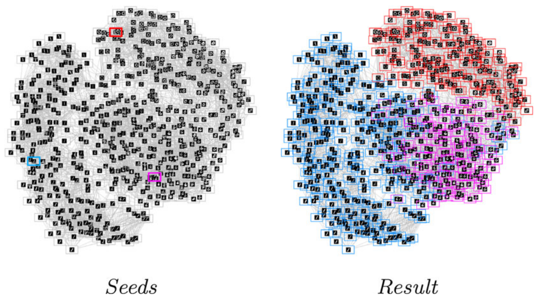

Fig. 9 Illustration of semi-supervised data clustering. The *left figure* (seeds) shows a graph built on a subset of the database of handwritten digits (0's, 1's, and 6's) with some nodes initially labelized (in *green*, *blue*, and *purple*) for each class. The *right figure* shows the results of the label diffusion on the graph. See text for more details (Color figure online)

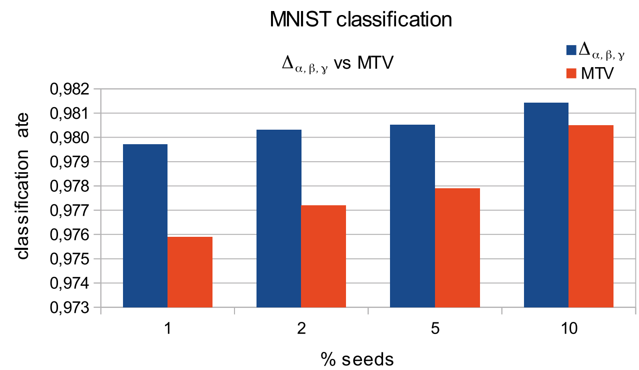

Fig. 10 Semi-supervised classification results for the MNIST database. The x-axis gives the amount of labelized vertices, and y-axis shows the classification rate. Best results were achieved using a local scaling parameter. See text for more details

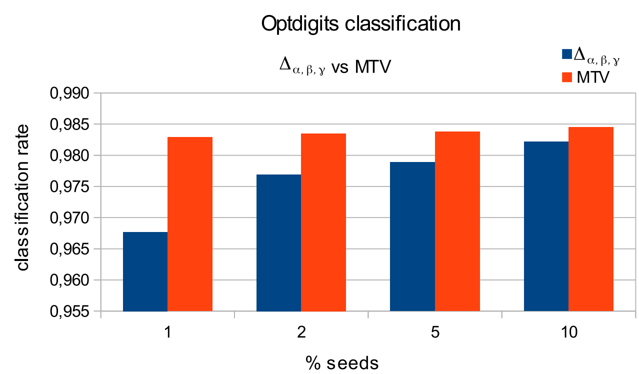

Fig. 11 Semi-supervised classification results. As in the case of the MNIST database, best results were achieved using a local scaling parameter. See text for more details

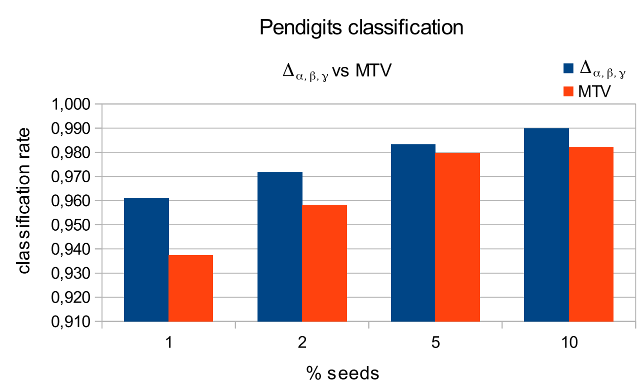

Fig. 12 Semi-supervised classification results for the PENDIGITS database. As for the cases of the MNIST and OPTDIGIT databases, best results were achieved using a local scaling parameter. See text for more details

in [13]. We perform our experiments in two different ways, depending on the databases:

- For the OPTDIGITS and PENDIGITS databases, we used a preprocessed version of the data, giving a constant size of feature vectors and invariance to small distortions (see [2] and [1] for more details on the preprocessing routines). We then determine the k-nearest neighbors of a node by using the Euclidean distance as metric.
- For the MNIST database, we use the original data from the database (for which the digits are stored as small images). To compute the k-nearest neighbors of a node, we used the two-sided tangent distance [41] as metric, which gives invariance to small affine transforms.

To compute weights for the edges between vertices, we use the Gaussian kernel similarity $w(u, v) = s_1(u, v)$ as discussed in Sect. 4.1, for which μ is the metric used during k-NN graph construction. Since the value choice of the variance parameter σ has a significant impact on the results, we consider two strategies to automatically compute its value: We use either a global scaling parameter $\sigma > 0$ or a local parameter σ_i for each vertex, as proposed in [73]. In this particular case, the similarity function becomes: $w(u, v) = \exp \frac{-\mu(u,v)^2}{\sigma_u \sigma_v}$, for which σ_u is the local scaling parameter at vertex u. We computed each σ_u as the distance to the Mth closest vertex to u. For the second strategy, we utilize a method proposed in [40]. The authors robustly estimate a global as well as a local σ parameter. In this work, we only use the global estimation, which is performed as: $\hat{\sigma} = 1.4826 median(||\mathcal{E}_S| - median|\mathcal{E}_S||)$, for which $\mathcal{E}_S$ is the set of local residuals in the graph computed as: $\mathcal{E}_u = (\sum_{v \sim u} f(u) - f(v))/\sqrt{|v \sim u|^2 + |v \sim u|}$ for a vertex u. For further details and justifications, see [40].

We can now apply the iteration scheme (99) to perform clustering on the discussed digit databases. For testing, we perform ten runs for each algorithm and we use a fixed percentage of already labelized vertices, whose positions are set randomly for each run. A typical labeling result is shown in Fig. 9. To evaluate our method, we compare the proposed method with the most effective method in the literature called multiclass total variation clustering (MTV) [13]. We show results for an optimized choice of parameters α, β, γ. As can be seen from the results on the MNIST (Fig. 10) and PENDIGITS (Fig. 12) databases, our method outperforms the state-of-the-art method, while for OPTDIGITS (Fig. 11) the results are a little bit worse, but comparable.

5 Conclusion

In this paper, we have introduced a novel family of graph p-Laplacian operators with gradient terms. These partial difference operators interpolate between nonlocal ∞-Laplacian, nonlocal Laplacian, and gradient terms on graphs. We considered an associated Dirichlet problem for this class of operators and have proven the existence and uniqueness of respective solutions. We also investigated the connections between the respective PdEs, nonlocal continuous PDEs, and stochastic Tug-of-War games. Finally, we have demonstrated the applicability of these operators in terms of a unified framework to solve many inverse problems in image processing, 3D point cloud processing, and machine learning.

Acknowledgments AE is supported by the ANR GRAPHSIP, and MT is supported by a European FEDER Grant (PLANUCA Project).

References

1. Alpaydin, E., Alimoglu, F.: Pen-based Recognition of Handwritten Digits Data Set. University of California, Irvine, Machine Learning Repository (1998)
2. Alpaydin, E., Kaynak, C.: Optical Recognition of Handwritten Digits Data Set. UCI Machine Learning Repository (1998)
3. Andreu, F., Mazón, J., Rossi, J., Toledo, J.: A nonlocal p-Laplacian evolution equation with Neumann boundary conditions. J. Math. Pures Appl. **90**(2), 201–227 (2008)
4. Andreu-Vaillo, F., Mazón, J.M., Rossi, J.D., Toledo-Melero, J.J.: Nonlocal Diffusion Problems, vol. 165. American Mathematical Society, Rhode Island (2010)
5. Arias, P., Facciolo, G., Caselles, V., Sapiro, G.: A variational framework for exemplar-based image inpainting. Int. J. Comput. Vis. **93**(3), 319–347 (2011)
6. Arya, S., Mount, D.M., Netanyahu, N.S., Silverman, R., Wu, A.Y.: An optimal algorithm for approximate nearest neighbor searching fixed dimensions. J. ACM **45**(6), 891–923 (1998). doi:10.1145/293347.293348
7. Bai, X., Sapiro, G.: Geodesic matting: a framework for fast interactive image and video segmentation and matting. Int. J. Comput. Vis. **82**(2), 113–132 (2009)
8. Bertalmio, M., Sapiro, G., Caselles, V., Ballester, C.: Image inpainting. In: Proceedings of the 27th Annual Conference on Computer Graphics and Interactive Techniques, pp. 417–424. ACM Press/Addison-Wesley Publishing Co. (2000)
9. Bertozzi, A.L., Flenner, A.: Diffuse interface models on graphs for classification of high dimensional data. Multisc. Model. Simul. **10**(3), 1090–1118 (2012)
10. Bertrand, G.: On topological watersheds. J. Math. Imaging Vis. **22**(2–3), 217–230 (2005)
11. Bougleux, S., Elmoataz, A., Melkemi, M.: Local and nonlocal discrete regularization on weighted graphs for image and mesh processing. Int. J. Comput. Vis. **84**(2), 220–236 (2009)
12. Boykov, Y.Y., Jolly, M.P.: Interactive graph cuts for optimal boundary & region segmentation of objects in nd images. In: Eighth IEEE International Conference on Computer Vision, 2001. ICCV 2001. Proceedings, vol. 1, pp. 105–112. IEEE (2001)
13. Bresson, X., Thomas, L., Uminsky, D., von Brecht, J.H.: Multiclass total variation clustering. In: Burges, C.J.C., Bottou, L., Ghahramani, Z., Weinberger, K.Q. (eds.) NIPS, pp. 1421–1429 (2013)
14. Buades, A., Coll, B., Morel, J.M.: Nonlocal image and movie denoising. Int. J. Comput. Vis. **76**(2), 123–139 (2008)
15. Bühler, T., Hein, M.: Spectral clustering based on the graph p-laplacian. In: Proceedings of the 26th Annual International Conference on Machine Learning, pp. 81–88. ACM (2009)
16. Chambolle, A., Lindgren, E., Monneau, R.: The Hölder infinite Laplacian and Hölder extensions. ESAIM Contr. Optim. CA. **18**(3), 799–835 (2012)
17. Chan, T.F., Kang, S.H., Shen, J.: Euler's elastica and curvature-based inpainting. SIAM J. Appl. Math. **63**(2), 564–592 (2003)
18. Coifman, R.R., Maggioni, M.: Diffusion wavelets. Appl. Comput. Harmon. Anal. **21**(1), 53–94 (2006)
19. Couprie, C., Grady, L., Najman, L., Talbot, H.: Power watershed: a unifying graph-based optimization framework. IEEE Trans. Pattern Anal. Mach. Intell. **33**(7), 1384–1399 (2011)
20. Cousty, J., Bertrand, G., Najman, L., Couprie, M.: Watershed cuts: minimum spanning forests and the drop of water principle. IEEE Trans. Pattern Anal. Mach. Intell. **31**(8), 1362–1374 (2009)
21. Criminisi, A., Pérez, P., Toyama, K.: Region filling and object removal by exemplar-based image inpainting. IEEE Trans. Image Process. **13**(9), 1200–1212 (2004)
22. Desquesnes, X., Elmoataz, A., Lézoray, O.: Eikonal equation adaptation on weighted graphs: fast geometric diffusion process for local and non-local image and data processing. J. Math. Imaging Vis. **46**(2), 238–257 (2013)
23. Drábek, P.: The p-Laplacian–Mascot of nonlinear analysis. Acta Math. Univ. Comen. **76**(1), 85–98 (2007)
24. Efros, A.A., Leung, T.K.: Texture synthesis by non-parametric sampling. In: The Proceedings of the Seventh IEEE International Conference on Computer Vision, 1999, vol. 2, pp. 1033–1038. IEEE (1999)
25. Elmoataz, A., Desquesnes, X., Lakhdari, Z., Lézoray, O.: Nonlocal infinity Laplacian equation on graphs with applications in image processing and machine learning. Math. Comput. Simul. **102**, 153–163 (2014)
26. Elmoataz, A., Desquesnes, X., Lézoray, O.: Non-local morphological PDEs and-Laplacian equation on graphs with applications in image processing and machine learning. IEEE J. Sel. Top. Signal Process. **6**(7), 764–779 (2012)
27. Elmoataz, A., Lezoray, O., Bougleux, S.: Nonlocal discrete regularization on weighted graphs: a framework for image and manifold processing. IEEE Trans. Image Process. **17**(7), 1047–1060 (2008)
28. Elmoataz, A., Lézoray, O., Bougleux, S., Ta, V.T.: Unifying local and nonlocal processing with partial difference operators on weighted graphs. In: International Workshop on Local and Non-local Approximation in Image Processing, pp. 11–26 (2008)
29. Elmoataz, A., Toutain, M., Tenbrinck, D.: On the p-Laplacian and ∞-Laplacian on graphs with applications in image and data processing. SIAM J. Imaging Sci. **8**(4), 2412–2451 (2015)
30. Falcão, A.X., Stolfi, J., de Alencar Lotufo, R.: Alencar Lotufo, R.: The image foresting transform: theory, algorithms, and applications. IEEE Trans. Pattern Anal. Mach. Intell. **26**(1), 19–29 (2004)
31. Ghoniem, M., Chahir, Y., Elmoataz, A.: Nonlocal video denoising, simplification and inpainting using discrete regularization on graphs. Signal Process. **90**(8), 2445–2455 (2010). doi:10.1016/j.sigpro.2009.09.004

32. Ghoniem, M., Elmoataz, A., Lezoray, O.: Discrete infinity harmonic functions: towards a unified interpolation framework on graphs. In: 2011 18th IEEE International Conference on Image Processing (ICIP), pp. 1361–1364. IEEE (2011)
33. Gilboa, G., Osher, S.: Nonlocal linear image regularization and supervised segmentation. Multisc. Model. Simul. **6**(2), 595–630 (2007)
34. Gilboa, G., Osher, S.: Nonlocal operators with applications to image processing. Multisc. Model. Simul. **7**(3), 1005–1028 (2008)
35. Grady, L.: Random walks for image segmentation. IEEE Trans. Pattern Anal. Mach. Intell. **28**(11), 1768–1783 (2006)
36. Hein, M., Bühler, T.: An inverse power method for nonlinear eigenproblems with applications in 1-spectral clustering and sparse PCA. In: Advances in Neural Information Processing Systems, pp. 847–855 (2010)
37. Johnson, A., Hebert, M.: Using spin images for efficient object recognition in cluttered 3d scenes. IEEE Trans. Pattern Anal. **21**(5), 433–449 (1999)
38. Kawohl, B.: Variations on the p-laplacian. In: Bonheure, D., Takac, P., et al. (eds.) Nonlinear Elliptic Partial Differential Equations. Contemporary Mathematics, vol. 540, pp. 35–46 (2011)
39. Kawulok, M., Smolka, B.: Texture-adaptive image colorization framework. EURASIP J. Adv. Signal Process. **2011**, 99 (2011)
40. Kervrann, C.: An adaptive window approach for image smoothing and structures preserving. In: Pajdla, T., Matas, J. (eds.) ECCV (3), Lecture Notes in Computer Science, vol. 3023, pp. 132–144. Springer (2004)
41. Keysers, D., Dahmen, J., Theiner, T., Ney, H.: Experiments with an extended tangent distance. In: ICPR, pp. 2038–2042 (2000)
42. LeCun, Y., Cortes, C.: MNIST handwritten digit database. http://yann.lecun.com/exdb/mnist/ (2010)
43. Lee, Y.S., Chung, S.Y.: Extinction and positivity of solutions of the p-Laplacian evolution equation on networks. J. Math. Anal. Appl. **386**(2), 581–592 (2012)
44. Leifman, G., Tal, A.: Mesh colorization. Comput. Graph. Forum **31**(2), 421–430 (2012). http://dblp.uni-trier.de/db/journals/cgf/cgf31.html#LeifmanT12
45. Leifman, G., Tal, A.: Pattern-driven colorization of 3d surfaces. In: CVPR, pp. 241–248 (2013)
46. Levin, A., Lischinski, D., Weiss, Y.: Colorization using optimization. ACM Trans. Graph. **23**(3), 689–694 (2004). doi:10.1145/1015706.1015780
47. Lindqvist, P.: Notes on the p-Laplace equation. Univ. (2006)
48. Lozes, F., Elmoataz, A., Lézoray, O.: Nonlocal processing of 3d colored point clouds. In: 2012 21st International Conference on Pattern Recognition (ICPR), pp. 1968–1971 (2012)
49. Lozes, F., Elmoataz, A., Lezoray, O.: Partial difference operators on weighted graphs for image processing on surfaces and point clouds. IEEE Trans. Image Process. **23**(9), 3896–3909 (2014). doi:10.1109/TIP.2014.2336548
50. Manfredi, J.J., Parviainen, M., Rossi, J.D.: Dynamic programming principle for tug-of-war games with noise. ESAIM Control Optim. Calc. Var. **18**(01), 81–90 (2012)
51. Manfredi, J.J., Parviainen, M., Rossi, J.D.: On the definition and properties of p-harmonious functions. Annali della Scuola Normale Superiore di Pisa-Classe di Scienze-Serie V **11**(2), 215 (2012)
52. Markle, W.: The development and application of colorization. SMPTE J. **93**(7), 632–635 (1984)
53. Meyer, F.: Topographic distance and watershed lines. Signal Process. **38**(1), 113–125 (1994)
54. Mitra, N.J., Nguyen, A., Guibas, L.: Estimating surface normals in noisy point cloud data. Int. J. Comput. Geom. Appl. **14**(04–05), 261–276 (2004)
55. Neuberger, J.M.: Nonlinear elliptic partial difference equations on graphs. Exp. Math. **15**(1), 91–107 (2006)
56. Osher, S., Fedkiw, R.: Level Set Methods and Dynamic Implicit Surfaces, vol. 153. Springer Science & Business Media (2006)
57. Park, J.H., Chung, S.Y.: Positive solutions for discrete boundary value problems involving the p-Laplacian with potential terms. Comput. Math. Appl. **61**(1), 17–29 (2011)
58. Peres, Y., Pete, G., Somersille, S.: Biased tug-of-war, the biased infinity Laplacian, and comparison with exponential cones. Calc. Var. Partial Differ. Equ. **38**(3–4), 541–564 (2010)
59. Peres, Y., Schramm, O., Sheffield, S., Wilson, D.: Tug-of-war and the infinity Laplacian. J. Am. Math. Soc. **22**(1), 167–210 (2009)
60. Peres, Y., Sheffield, S., et al.: Tug-of-war with noise: a game-theoretic view of the p-laplacian. Duke Math. J. **145**(1), 91–120 (2008)
61. Rusu, R.B., Blodow, N., Marton, Z.C., Beetz, M.: Aligning point cloud views using persistent feature histograms. In: IEEE/RSJ International Conference on Intelligent Robots and Systems, 2008. IROS 2008, pp. 3384–3391. IEEE (2008)
62. Schnabel, R., Wahl, R., Klein, R.: Efficient ransac for point-cloud shape detection. In: Computer Graphics Forum, vol. 26, pp. 214–226. Wiley Online Library (2007)
63. Schönlieb, C.B., Bertozzi, A.: Unconditionally stable schemes for higher order inpainting. Commun. Math. Sci. **9**(2), 413–457 (2011)
64. Sethian, J.A.: Level set methods and fast marching methods: evolving interfaces in computational geometry, fluid mechanics, computer vision, and materials science. In: Cambridge Monographs on Applied and Computational Mathematics. Cambridge University Press, Cambridge (1999)
65. Sinop, A.K., Grady, L.: A seeded image segmentation framework unifying graph cuts and random walker which yields a new algorithm. In: IEEE 11th International Conference on Computer Vision, 2007. ICCV 2007, pp. 1–8. IEEE (2007)
66. Sýkora, D., Buriánek, J., Žára, J.: Unsupervised colorization of black-and-white cartoons. In: NPAR, pp. 121–128 (2004)
67. Ta, V.T., Elmoataz, A., Lézoray, O.: Adaptation of eikonal equation over weighted graph. In: Scale Space and Variational Methods in Computer Vision, pp. 187–199. Springer, Berlin, Heidelberg (2009)
68. Ta, V.T., Elmoataz, A., Lézoray, O.: Nonlocal PDEs-based morphology on weighted graphs for image and data processing. IEEE Trans. Image Process. **20**(6), 1504–1516 (2011)
69. Toutain, M., Elmoataz, A., Lozes, F., Mansouri, A.: Non-local discrete ∞-Poisson and Hamilton Jacobi equations—from stochastic game to generalized distances on images, meshes, and point clouds. J. Math. Imaging Vis. **55**(2), 229–241 (2016). doi:10.1007/s10851-015-0592-x
70. Vincent, L., Soille, P.: Watersheds in digital spaces: an efficient algorithm based on immersion simulations. IEEE Trans. Pattern Anal. Mach. Intell. **13**(6), 583–598 (1991)
71. Von Luxburg, U.: A tutorial on spectral clustering. Stat. Comput. **17**(4), 395–416 (2007)
72. Yatziv, L., Sapiro, G.: Fast image and video colorization using chrominance blending. IEEE Trans. Image Process. **15**(5), 1120–1129 (2006)
73. Zelnik-manor, L., Perona, P.: Self-tuning spectral clustering. In: Advances in Neural Information Processing Systems, vol. 17, pp. 1601–1608. MIT Press (2005)
74. Zhou, D., Schölkopf, B.: Discrete regularization. In: Semi-Supervised Learning, pp. 221–232. MIT Press (2006)

Abderrahim Elmoataz is a full professor of Computer Science at the Université de Caen Normandy, France. His research concerns partial differential equations (PDEs) on 3-D surfaces and points clouds, PDEs on graphs of arbitrary topology with applications in image processing, and machine learning.

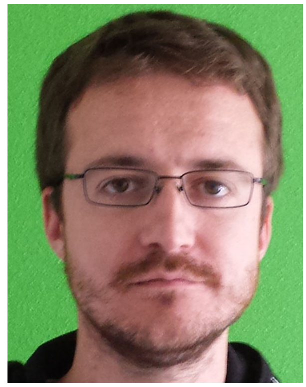

Matthieu Toutain received the M.Sc. and Doctoral degree in Computer Science from the University of Caen, Normandy, France in 2011 and 2015, respectively. His research mainly concerns image and data processing with graph-based variational and morphological methods.

François Lozes received his Ph.D. degree in Computer Science at the Université de Caen Basse-Normandie, France. His research mainly concerns the analysis of data on 3-D meshes and 3-D point clouds using graph signal processing.